Midlatitude shelf seas in the Cenomanian-Turonian greenhouse world: Temperature evolution and North Atlantic circulation

Silke Voigt
Geological Institute, University of Cologne, Köln, Germany

Andrew S. Gale[1]
Department of Earth and Environmental Sciences, University of Greenwich, Chatham Maritime, Kent, UK

Sascha Flögel
Leibnitz-Institut für Meereswissenschaften, Kiel, Germany

Received 15 February 2004; revised 7 September 2004; accepted 30 September 2004; published 8 December 2004.

[1] An 8 million year record of subtropical and midlatitude shelf-sea temperatures, derived from oxygen isotopes of well-preserved brachiopods from a variety of European sections, demonstrates a long-term Cenomanian temperature rise (16–20°C, midlatitudes) that reached its maximum early in the late Turonian (23°C, midlatitudes). Superimposed on the long-term trend, shelf-sea temperatures vary at shorter timescales in relation to global carbon cycle perturbations. In the mid-Cenomanian and the late Turonian, two minor shelf-sea cooling events (2–3°C) coincide with carbon cycle perturbations and times of high-amplitude sea level falls. Although this evidence supports the hypothesis of potential glacioeustatic effects on Cretaceous sea level, the occurrence of minimum shelf-sea temperatures within transgressive beds argues for regional changes in shelf-sea circulation as the most plausible mechanism. The major carbon cycle event in the latest Cenomanian (oceanic anoxic event 2) is accompanied by a substantial increase in shelf-sea temperatures (4–5°C) that occurred ~150 kyr after the commencement of the $\delta^{13}C$ excursion and is related to the spread of oceanic conditions in western European shelf-sea basins. Our oxygen isotope record and published $\delta^{18}O$ data of pristinely preserved foraminifera allow the consideration of North Atlantic surface water properties in the Cenomanian along a transect from the tropics to the midlatitudes. On the basis of fossil-derived $\delta^{18}O$, estimated δw ranges, and modeled salinities, temperature-salinity-density ranges were estimated for tropical, subtropical, and midlatitude surface waters. Accordingly, the Cenomanian temperate shelf-seas waters have potentially the highest surface water density and could have contributed to North Atlantic intermediate to deep waters in the preopening stage of the equatorial Atlantic gateway. *INDEX TERMS:* 9609 Information Related to Geologic Time: Mesozoic; 4267 Oceanography: General: Paleoceanography; 9325 Information Related to Geographic Region: Atlantic Ocean; 4870 Oceanography: Biological and Chemical: Stable isotopes; 4283 Oceanography: General: Water masses; *KEYWORDS:* Cretaceous, Cenomanian, Turonian, shelf-sea temperatures, brachiopods, stable isotopes

Citation: Voigt, S., A. S. Gale, and S. Flögel (2004), Midlatitude shelf seas in the Cenomanian-Turonian greenhouse world: Temperature evolution and North Atlantic circulation, *Paleoceanography*, *19*, PA4020, doi:10.1029/2004PA001015.

1. Introduction

[2] The Mesozoic-Cenozoic greenhouse climate peaked during Cenomanian-Turonian times and reached its thermal maximum during the late Turonian [*Clarke and Jenkyns*, 1999; *Wilson et al.*, 2002]. Unusually warm sea surface temperatures (SST) were reported for the tropical (33–34°C) [*Norris et al.*, 2002; *Wilson et al.*, 2002; *Schouten et al.*, 2003], and southern subpolar Atlantic Ocean (30–32°C) [*Bice et al.*, 2003], based on oxygen isotope data from glassy foraminifera and archaeal membrane lipids, and are interpreted to be the consequence of intensified meridional heat transport caused by increased greenhouse gas forcing and accelerated ocean crust production [*Larson*, 1991]. However, evidence of SSTs warmer than 32°C are only snapshots of Cenomanian-Turonian time. A first paleotemperature record with a high temporal resolution from the late Albian to the earliest Cenomanian shows pronounced short-term variability (10–100 kyr) in both SSTs and the thermal structure of the surface ocean, suggesting a highly dynamic ocean hydrology during greenhouse climate conditions [*Wilson and Norris*, 2001].

[3] Opposing the evidence for extraordinarily warm tropics, a variety of authors have repeatedly suggested that short glaciations (<100 kyr) may have occurred within the ice-free Cenomanian-Maastrichtian greenhouse world, based on correlation between shallow water sequences

[1]Also at Department of Palaeontology, Natural History Museum, London, UK.

0883-8305/04/2004PA001015

and $\delta^{18}O$-derived paleotemperature records [*Miller et al.*, 1999, 2003; *Stoll and Schrag*, 2000]. In Cenomanian time, third- and fourth-order sea level changes were eustatic and occurred synchronously within the resolution of ammonite biozones [*Gale et al.*, 2002]. Glacioeustasy is the only known mechanism that can drive large (amplitudes >10 m) and rapid (<100 kyr) sea level changes [*Pitman and Golovchenko*, 1983]. However, evidence for glacioeustasy in Cenomanian-Turonian times is complicated either by low temporal resolution of deep-sea $\delta^{18}O$ records, which do not resolve variations at timescales less than 100 kyr [e.g., *Huber et al.*, 2002], or by diagenetic alteration of bulk carbonate $\delta^{18}O$ data [e.g., *Clarke and Jenkyns*, 1999; *Stoll and Schrag*, 2000]. Additionally, uncertainties in correlations along coast-shelf-ocean transects at timescales of less than 100 kyr have so far inhibited the direct comparison of sea level and paleotemperature records.

[4] During Cenomanian-Turonian times, three positive carbon isotope excursions indicate a major and two minor perturbations in the global carbon cycle. The Cenomanian-Turonian Boundary Event (CTBE) is one of the major Mesozoic events (2–3‰ positive $\delta^{13}C$ excursion; *Scholle and Arthur* [1980]) related to enhanced rates of organic carbon burial, widespread oceanic anoxia (oceanic anoxic event 2 (OAE 2) of *Schlanger and Jenkyns* [1976]), the demise of tropical carbonate platforms and major faunal changes. The proposed climate response to this event includes substantial cooling as a consequence of enhanced sequestration of organic carbon [*Arthur et al.*, 1988; *Kuypers et al.*, 1999] and the incursion of boreal faunas into low-latitude seas [*Kuhnt et al.*, 1986; *Gale and Christensen*, 1996] or pronounced warming of deep-sea and surface waters [*Luderer and Kuhnt*, 1997; *Huber et al.*, 1999]. The events in the earliest middle Cenomanian (MCE) and the late Turonian (LTE) are smaller in magnitude (1‰ positive $\delta^{13}C$ excursion), and are characterized by increases in bulk-carbonate oxygen isotopes and boreal migration in European shelf seas, which are interpreted to reflect pronounced climate cooling [*Paul et al.*, 1994; *Erbacher et al.*, 1996; *Stoll and Schrag*, 2000; *Voigt and Wiese*, 2000].

[5] Here we present an 8 million year record of mid-Cretaceous shelf-sea temperatures based on new and previously published oxygen isotopes of well-preserved brachiopod calcite from subtropical and temperate European basins [*Voigt*, 2000; *Voigt et al.*, 2003; S. Voigt et al., Chronology of short-termed sea-level, carbon cycle, and climate variations during the Cenomanian-Turonian boundary event in NW Europe, submitted to *Cretaceous Research*, 2004]. Low-magnesium calcite of brachiopod shells is the most suitable substrate to reconstruct the paleoceanographic history in shelf sea environments because of the complex history of early, burial and meteoric diagenesis of land sections. The record resolves pronounced short-term temperature variations (in the order of 100 kyr) through Cenomanian-Turonian carbon cycle events. In combination with $\delta^{18}O$-derived surface, thermocline and deep-sea temperatures from ODP sites, we discuss tropical, subtropical and midlatitude surface water properties. The record suggests that (1) the temperate midlatitudes shelf-seawaters could have contributed to Cenomanian intermediate to deep waters, and (2) Cenomanian-Turonian carbon cycle perturbations occurred concomitant to high-amplitude sea level changes, whereby falling and rising sea level is related to decreasing and rising shelf-sea temperatures.

2. Material and Methods

[6] A composite of 24 different Cenomanian and Turonian sections from midlatitude (~35–36°N paleolatitude) and subtropical (26–28°N) European shelf-sea basins were sampled for specimens of articulate brachiopods (Figure 1; see auxiliary material[1]). Localities at midlatitudes are situated in southern England and northern Germany, with Cenomanian sample sites at Southerham, Eastbourne, Lydden Spout (England), and Quedlinburg (Germany), and Turonian sections at Dover, Kensworth, Lewes (southern England), Söhlde and Hoppenstedt (northern Germany). All successions expose a pelagic carbonate facies consisting of marly chalks, chalks and pelagic limestones. Subtropical localities are situated at the northern Tethys margin in northern Spain (North Cantabrian Basin) and southeastern France (Vocontian Basin). Sections in northern Spain expose a carbonate shelf in the Cenomanian and mixed hemipelagic silicilastics and carbonates in the Turonian [*Wilmsen et al.*, 1996]. Two localities in the Vocontian Basin expose a basinal marl-limestone facies (St. Lions) and a shallower transitional facies between platform carbonates and basinal marls (Col des Abesses).

[7] A total of 417 stratigraphically horizoned brachiopod shells were studied for their preservation and stable isotopic composition (for an overview of new and already published data see auxiliary material). The occurrence of distinct brachiopod species is frequently limited to certain stratigraphic horizons (e.g., acme occurrences of *Orbirhynchia mantelliana* in the early and middle Cenomanian [*Paul et al.*, 1994]). Therefore the composite Cenomanian-Turonian $\delta^{18}O$ record is based on different brachiopod taxa consisting of rhynchonellid (*Orbirhyncia*, *Grasirhynchia*, *Modestella*, *Gemmarcula*) and terebratulid (*Concinnthyris*, *Capillithyris*, *Kingena*, *Terebriostra*, *Terebratulina, Gibbithyris*) genera.

[8] The samples were mechanically scraped and cleaned in an ultrasonic bath to separate shell calcite from the adherent matrix. Polished thin sections were prepared from one half of the samples for conventional and cathodoluminescence microscopy (CL) carried out with a hot cathode luminescense microscope (HC1-LM). Selected shell samples were broken into small pieces, and their textural preservation was examined with a scanning electron microscope (SEM, CamScan CS44 ED). In order to perform element geochemistry and stable isotope analysis, about 1.5 mg of sample material was drilled from the best preserved domain of the fibrous secondary (all rhynchonellids and most terebratulids) or the prismatic tertiary (terebratulid genera *Concinnthyris* and *Gibbithyris*) shell layer using a binocular microscope. If both valves were preserved, the posterior part of the

[1] Auxiliary material is available at ftp://ftp.agu.org/apend/pa/2004PA001015.

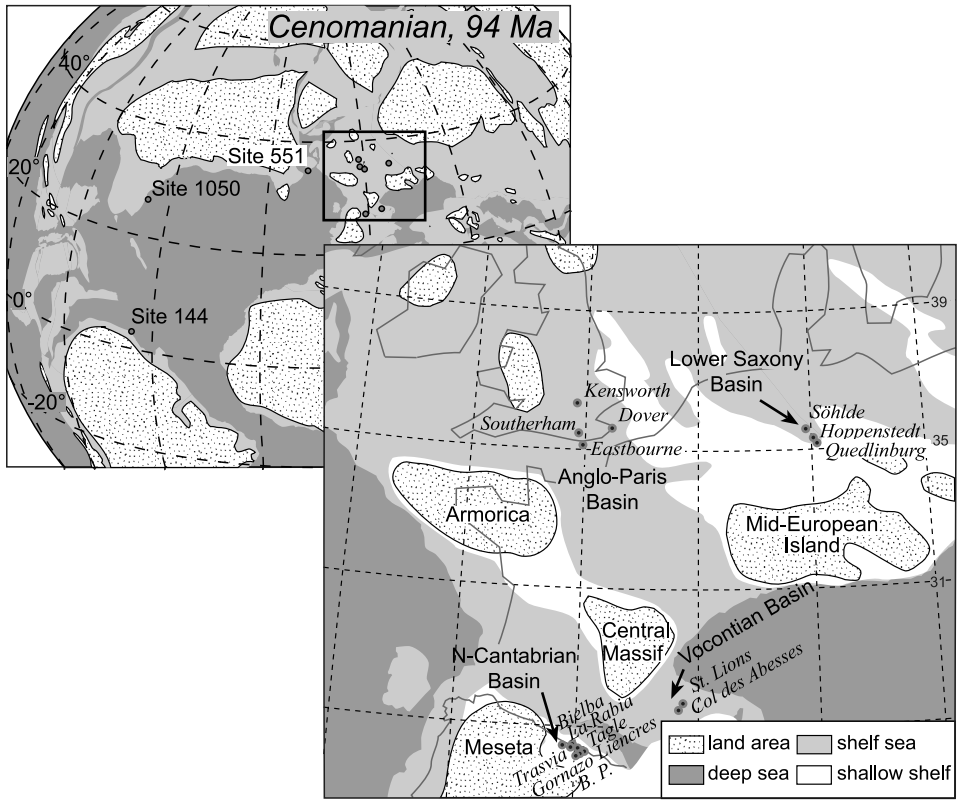

Figure 1. Cenomanian (94 Ma) paleogeography with localities in central and western Europe (this study) and the North Atlantic ocean (literature data from DSDP/ODP sites 144, 551, and 1050). B. P., Boo de Pielagos.

dorsal valve was used preferentially to avoid kinetic fractionation effects as described by *Curry and Fallick* [2002]. Element concentrations were measured with ICP-AES (Oldenburg) or ICP-MS (Cologne) by the reaction of 1 mg powder with 5% HNO_3, and determination of element concentrations for Mg, Fe, Mn, and Sr in μg/g. Stable isotope ratios were measured with a mass spectrometer of Analytical Precision (Jülich) coupled to an automatic preparation system. Values are given against the VPDB standard, and reproducibility of repeated standard measurements was better than 0.1‰ for carbon and 0.15‰ for oxygen.

[9] Temporal resolution of the composite brachiopod record depends on the abundance of brachiopods and the quality of interbasinal correlations, and ranges from the level of ammonite zones (northern Spain) to the level of orbital timescales (<100 kyr) in the middle and late Cenomanian and late Turonian (midlatitude localities, Figure 2). Cenomanian samples from midlatitude localities are calibrated against the orbitally tuned cyclostratigraphy of *Gale et al.* [1999], which has been fixed to the chronostratigraphic age of the C-T Boundary (93.5 Ma; *Gradstein et al.* [1995], FO *W. devonense*, *Q. gartneri*). The late Turonian age model is based on the highly coherent correlation of two continuous $\delta^{13}C$ records from a boreal (Salzgitter-Salder; *Voigt and Hilbrecht* [1997]) and a Tethyan (Contessa; *Stoll and Schrag* [2000]) section (Figure 2). The mean sedimentation rate is two times higher at Salzgitter-Salder (99.3 m/myr) than at Contessa (9.86 m/myr). Both records were interpolated between the ages for the middle-upper Turonian (FO *S. neptuni*, ~90.4 Ma) and the Turonian-Coniacian boundary (89.0 Ma) [*Gradstein et al.*, 1995]. Numerical ages were assigned to late Turonian brachiopods based on interpolation of carbon isotope stratigraphy and five bentonite layers, which occur in both southern England and northern Germany [*Wray*, 1999]. In the early to middle Turonian interval, strong biogeographic differentiation and a poor calibration of microfossil and macrofossil biozones with carbon isotope stratigraphy results in a higher degree of uncertainty of chronological ages. The estimated error is in the order of 100 to 500 kyr. Here the Contessa-$\delta^{13}C$ record has been interpolated between the ages of the Cenomanian-Turonian and middle-upper Turonian boundaries.

3. Preservation

[10] Macroscopic shell preservation ranges from moderate to very good, and is better in sections with chalks or platform carbonates than in hemipelagic chalks and calcareous siltstones. In order to evaluate the preservation state of the brachiopod shell calcite, an integrated approach of trace element geochemistry, SEM and CL microcopy is used. CL microscopy allows the identification of the best preserved domains of the brachiopod shells. Diagenetically unaltered low-Mg calcite appears nonluminescent, whereas early

diagenetic incorporation of Mn^{2+} in the calcite lattice acts as the most prominent activator of an orange-colored luminescence, which can be quenched by additional incorporation of Fe^{2+} [*Machel et al.*, 1991]. Both elements are enriched in fluids under reducing conditions, are common in early diagenetic environments, and may serve as indicator of diagenetic recrystallization of low-Mg calcite [*Veizer*, 1983]. In this study, brachiopod shells with less than

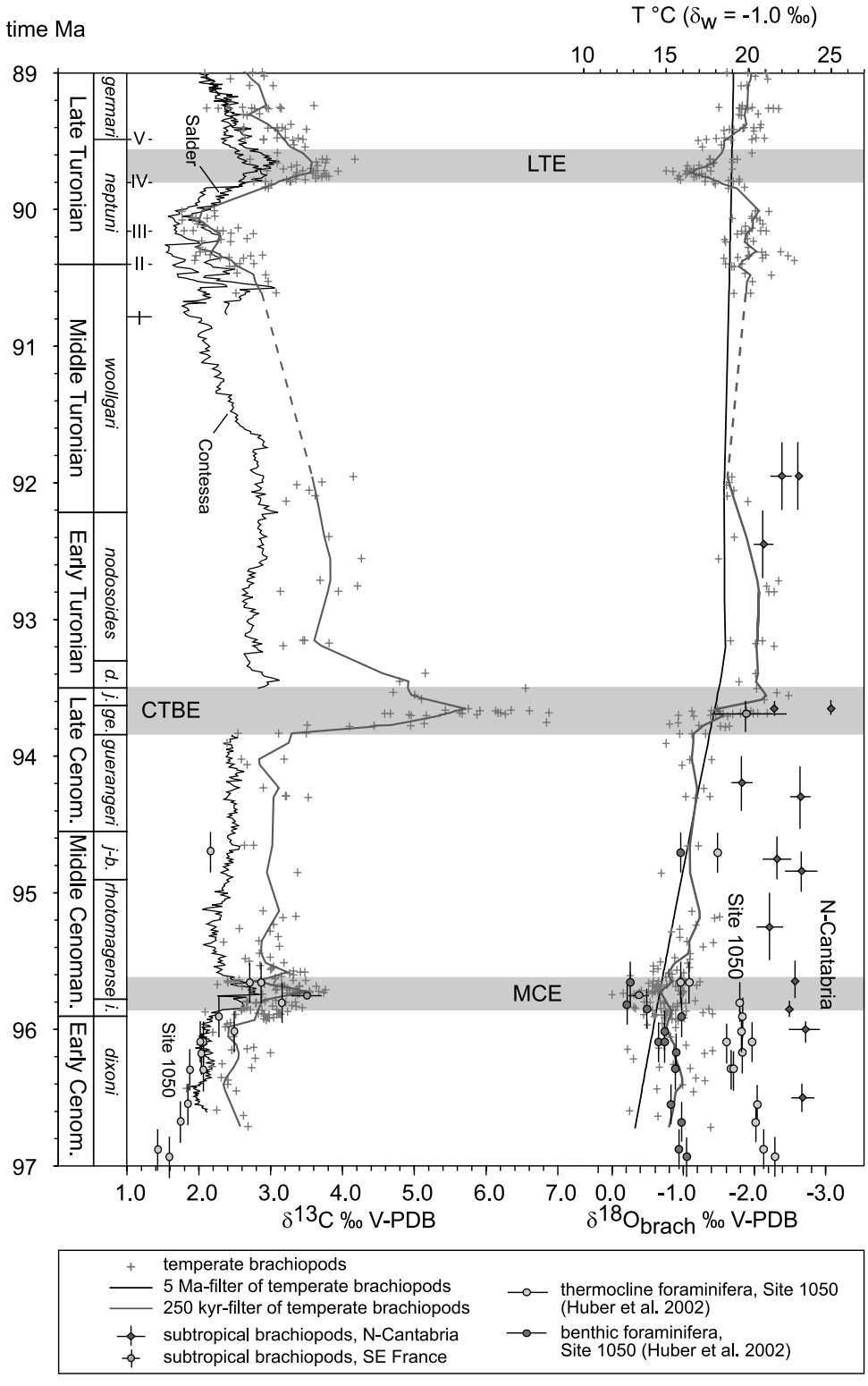

Figure 2

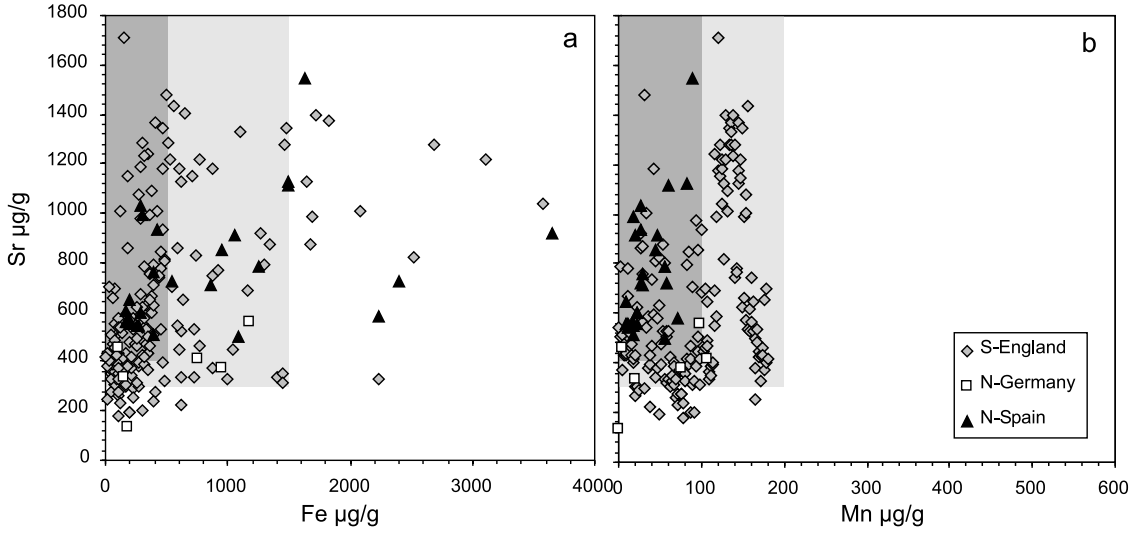

Figure 3. Trace element composition (Fe, Mn, Sr) of Cenomanian-Turonian brachiopods from southern England, northern Germany, and northern Spain. The dark gray area marks the range of modern brachiopods, and shell samples within this field are classified as very well preserved. The light gray area indicates good to moderately preserved shell calcites.

100 µg/g Mn and 500 µg/g Fe are considered to be very good preserved, whereas shells with Mn and Fe concentrations between 100 and 200 µg/g and 500 and 1500 µg/g are classified as good to moderately preserved (Figure 3).

[11] Independent of the redox state, postdepositional recrystallization causes a loss of strontium in skeletal calcite [*Veizer et al.*, 1986]. Primarily, incorporation of strontium into biogenic calcites is controlled by metabolic processes governing the rate of calcite precipitation, and by environmental conditions such as variations in seawater salinity, temperature and Sr/Ca ratio [*Klein et al.*, 1996; *Stanley and Hardie*, 1998; *Steuber*, 2002]. Modern brachiopods have a slow metabolism and a low rate of strontium uptake in the lattice of their secondary layer [*Curry et al.*, 1989; *Brand and Brenckle*, 2001; *Curry and Fallick*, 2002]. Strontium concentrations of recent brachiopods are between 450 and 1550 µg/g with a mean value of ~1000 µg/g [*Morrison and Brand*, 1986; *Brand et al.*, 2003]. The mean strontium concentration of Cenomanian-Turonian brachiopod shells is lower (700 µg/g) in comparison to modern values, but shows a large range of values from 200 to 1700 µg/g (Figure 3). The strontium concentration of brachiopod shells is also lower than strontium concentrations reported for mid-Cretaceous rudists and belemnites (1100–1500 µg/g; *Steuber and Veizer* [2002]). Low Sr concentrations in brachiopod shells can be either attributed to an early diagenetic loss or to a taxonomically mediated lower rate of strontium uptake (lower distribution coefficient). The large range of strontium concentrations in Cenomanian-Turonian brachiopod shells is related to a pronounced variability through time (Figure 4). The majority of Cenomanian-Turonian brachiopod shells have strontium concentrations between 300 and 700 µg/g, however, brachiopod specimens of early middle Cenomanian age have strontium concentrations, which are about three times higher (1200–1700 µg/g). The mid-Cenomanian brachiopod specimens do not differ in their structural and chemical shell preservation from other specimens of Cenomanian-Turonian age. Therefore it is not very reasonable to attribute the variability in strontium concentrations to different degrees of early diagenetic alteration. The substantial increase of strontium concentrations in the early middle Cenomanian, seems more to be related to environmental conditions, such as fast changes in the Sr/Ca ratio of seawater. It remains to be tested, if other taxonomical groups show similar temporal variations in their Sr/Ca ratios and if the low brachiopod strontium concentrations are biologically controlled. In order to take an early diagenetical loss of Sr into account, we used the lower value (400 µg/g) of the modern range to discriminate between good and moderately (300–400 µg/g) preserved brachiopod specimens.

Figure 2. Composite Cenomanian-Turonian carbon isotopes and paleotemperatures derived from $\delta^{18}O$ values of low- to middle-latitude brachiopods (this study) and subtropical planktonic and benthic foraminifera [*Huber et al.*, 2002]. Bulk carbonate $\delta^{13}C$ stratigraphies of Salder [*Voigt and Hilbrecht*, 1997] and Contessa [*Stoll and Schrag*, 2000] mark the position of the MCE, CTBE, and LTE. Roman letters indicate bentonites, which can be correlated between the Anglo-Paris and the north German basins (I-TC, Glynde Marl1; II-TC2, Southerham; III-TD, Caburn; IV-TE, Bridgewick 1; V-TF, Lewes) [*Wray*, 1999]. The timescale is from *Gradstein et al.* [1995]. All paleotemperature estimates use a conservative δ_w value of −1.0‰ for an ice-free world. Temperatures are calculated using the equations of *Anderson and Arthur* [1983] for brachiopods, of *Bemis et al.* [1998] for nonsymbiontic planktic foraminifera, and of *Shackleton* [1974] for benthic foraminifera.

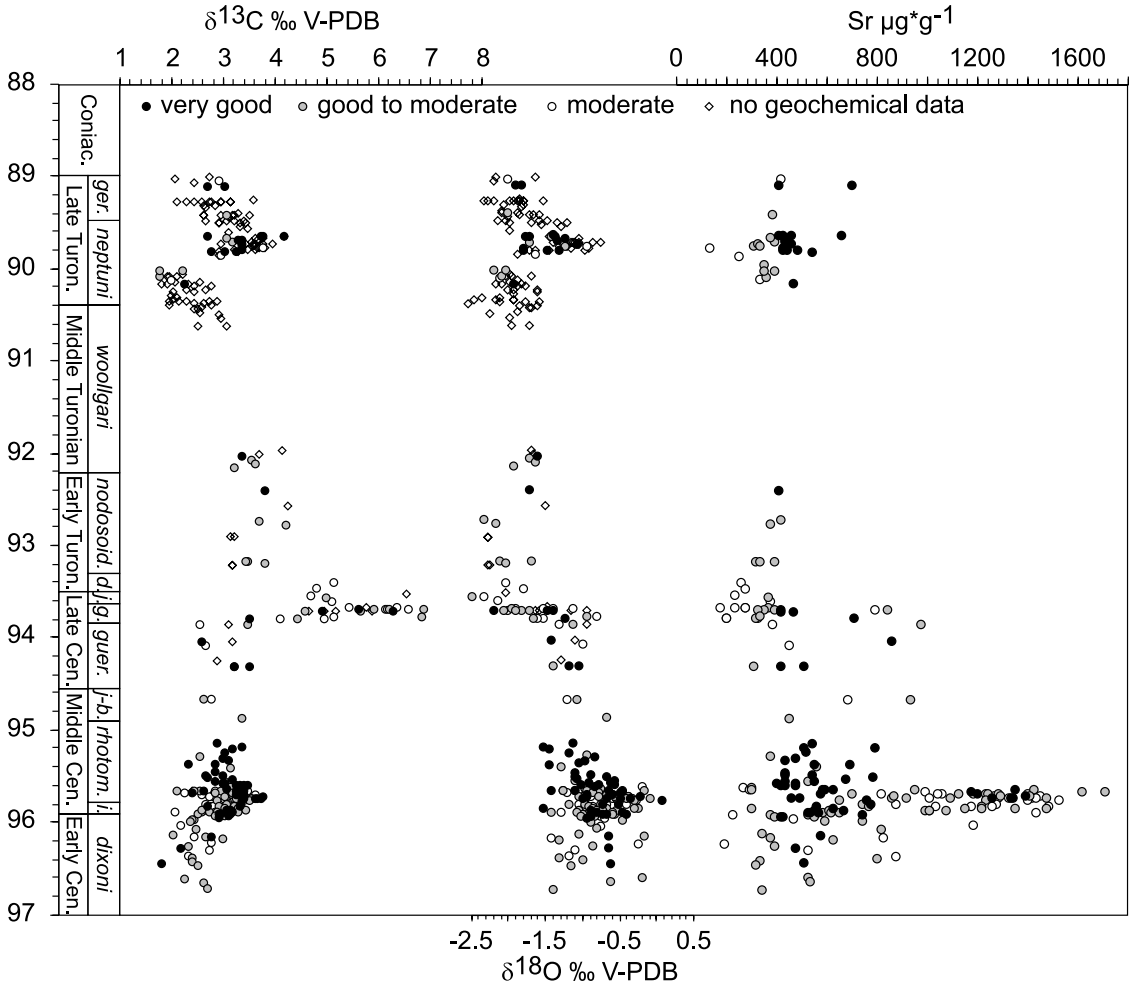

Figure 4. Stable carbon and oxygen isotopic composition and strontium concentrations of Cenomanian-Turonian temperate brachiopod shells with different degrees of preservation. Very good preserved shells match all geochemical screening criteria and appear nonluminescent (closed circles). Good to moderately preserved shells plot in the light gray field of Figure 3 and appear nonluminescent (gray circles). Moderately preserved shells do not match geochemical boundary conditions and show signs of weak luminescence (see Figure 5e, open circles). Carbon and oxygen isotope values do not show a systematic offset between very good and moderately preserved shells. Note the fast increase of strontium concentrations in the earliest middle Cenomanian, which probably reflects a sudden change in the seawater Sr/Ca ratio.

[12] The majority of studied brachiopod samples have nonluminescent secondary and tertiary shell layers (Figures 5a, 5b, 5c, 5d, and 5f). Some rhynchonellids show signs of secondary layer cementation in the space between calcitic fibres (Figure 5e). The hollows of terebratulid punctae are commonly filled with secondary cements, which is visible in the texture (Figures 5g and 5i) and by the orange luminescence (Figure 5c). To minimize the influence of cemented punctae, the posterior part of the brachiopod shell was chosen for sampling. Punctae are small in this shell domain and hold only a minor portion of the shell calcite (< 5%). Rhynchonellid brachiopod shells are best preserved in the posterior shell portion as well.

[13] About 70% of all studied brachiopod shells are classified as very good to good preserved and their isotopic composition as primary. Moderately preserved shells do not match all geochemical screening criteria, but are usually not significantly offset in their stable isotopic composition from the good and very good preserved shells (Figure 4). Oxygen and carbon isotope values of moderately preserved shells show a broader scatter during certain time intervals, but are not systematically enriched or depleted. In oder to enhance the stratigraphic resolution, we do not exclude moderate shells from the data base, but discuss their isotopic signature only in terms of mean values.

4. Equilibrium Precipitation

[14] The first systematic isotopic study of brachiopod shells goes back to the work of *Lowenstam* [1961], who

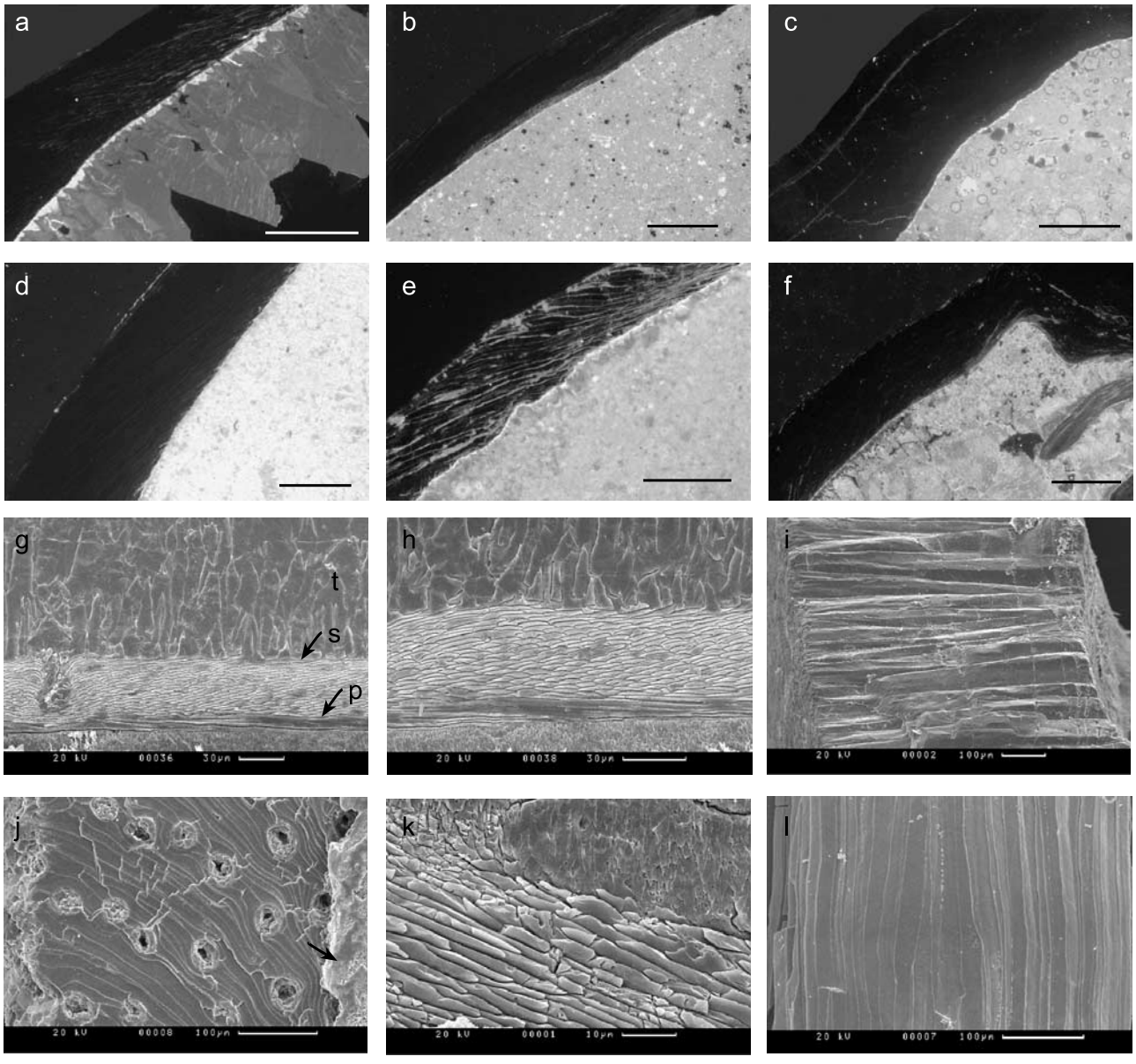

Figure 5. CL and SEM images of rhynchonellid and terebratulid brachiopods showing the preservation state of shell calcite: (a) nonluminescent shell of the rhynchonellid species *Orbirhynchia mantelliana* (Southerham, middle Cenomanian) with different generations of luminescent sparite (sample S4), (b) nonluminescent secondary shell layer of *Grasirhynchia grasiana* (Southerham, lower Cenomanian, sample S44), (c) nonluminescent shell of *Gibbithyris* (Hoppenstedt, lower Turonian) with small cement-filled luminescent punctae, (d) well-preserved nonluminescent shell of *Orbirhynchia multicostata* (Eastbourne, upper Cenomanian, sample Hw4), (e) moderately preserved shell of *Orbirhynchia multicostata*, which is from the same bed as Figure 5d (sample Hw5), (f) nonluminescent shell and luminescent brachidium of *Orbirhynchia multicostata* (Eastbourne, upper Cenomanian, sample E31b), scale bar for all CL images is 0.5 cm, (g) primary (p), fibrous secondary (s), and prismatic tertiary (t) shell layer of *Concinnithyris subundata* (sample D1, Dover, middle Cenomanian), (h) detail of Figure 5g, (i) tertiary layer of a well-preserved shell of *Gibbithyris* (Hoppenstedt, lower Turonian, sample Hb1), (j) very well preserved secondary layer of the terebratulid genus *Concinnithyris* (Dover, middle Cenomanian) overlain by the recrystallized primary layer (arrow), punctae are partly cemented (sample LS20), (k) well-preserved secondary layer of the rhynchonellid genus *Monticlarella* (Southerham, lower Cenomanian, sample S25), (l) well-preserved fibrous secondary layer of *Orbirhynchia mantelliana* (Dover, middle Cenomanian, sample LS8).

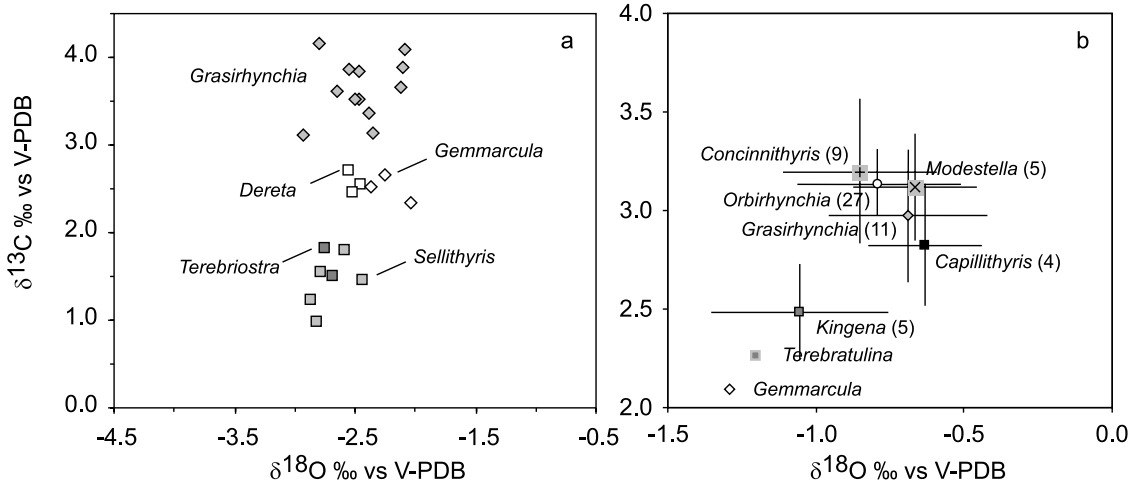

Figure 6. The $\delta^{18}O$-$\delta^{13}C$ cross plots of different middle to late Cenomanian genera demonstrate taxon-related metabolic effects. (a) Data from the 96–94 Myr interval in northern Spain. The terebratulid genera *Terebriostra*, *Sellithyris*, *Dereta*, and *Gemmearcula* are depleted in ^{13}C by 1–2‰ in comparison to the rhynchonellid genus *Grasirhynchia*. (b) Mean $\delta^{18}O$ and $\delta^{13}C$ values of eight genera with 1σ standard deviations (error bars, bracketed numbers are number of specimens) from couplets B35–B40 and C2–C10 (~150 kyr before and after the MCE) in southern England. The genera *Orbirhynchia*, *Grasirhynchia* (both rhynchonellid), *Concinnithyris*, *Capillithyris*, and *Modestella* (all terebratulid) show a narrow range of $\delta^{13}C$ and $\delta^{18}O$ values. The terebratulid genera *Terebratulina*, *Kingena*, and *Gemmarcula* are depleted in ^{13}C and ^{18}O by 0.5–1.0‰.

measured the oxygen isotopic composition of different species of all modern superfamilies at different latitudes and corresponding water samples, and found the $^{18}O/^{16}O$ ratio of brachiopod shells strongly to be related to seawater temperature but not to species. Later, *Carpenter and Lohmann* [1995] demonstrated substantial deviations from seawater isotopic equilibrium for the primary shell layer and specialized portions of the brachiopod shell as brachidium, foramen, and muscle scars. However, the isotopic composition of the secondary shell layer were found to be close to the isotopic equilibrium, a result that was reproduced for the species *Laqueus californianus* [*Buening and Spero*, 1996] and for four terebratulid species from the Lacepede shelf in Australia [*James et al.*, 1997]. More recently, isotopic studies on specimens of single species have shown substantial offsets from the isotopic equilibrium. *Curry and Fallick* [2002] found systematic differences in the oxygen isotope ratio of matching dorsal and ventral valves for the terebratulid species *Calloria inconspicua* (Sowerby), with the thinner dorsal valve yielding the higher and less variable $\delta^{18}O$ values. *Auclair et al.* [2003] demonstrated seasonal variable kinetic fractionation effects for the primary and the upper secondary layer of *Terebratalia transversa* (Sowerby), with deviations from isotopic equilibrium of up to 6‰. Owing to the limited numer of recent studies so far, it remains to be tested whether kinetic disequilibrium precipitation of brachiopod shells is restricted to certain taxonomic groups or to environmental conditions, and how the isotopic composition of fossil brachiopods is affected.

[15] In order to test the possibility of metabolic fractionation effects for Cenomanian-Turonian brachiopods, we compared the $\delta^{13}C$ and $\delta^{18}O$ values of different genera from middle to late Cenomanian localities in northern Spain and southern England (Figure 6). Middle to late Cenomanian terebratulid brachiopods from northern Spain are depleted in ^{13}C by 1.0‰ (*Dereta*, *Gemmarcula*) to 2.0‰ (*Terebriostra*, *Sellithyris*) in comparison to the rhynchonellid genus *Grasirhynchia*. However, the oxygen isotopic composition of these genera shows only a small offset of less than 0.5‰ (Figure 6a). The abundant occurrence of a diverse mid-Cenomanian brachiopod fauna in southern England allows the comparison of eight genera within a relatively short period of time (~500 kyr). We used specimens from the interval before (couplets B35–B40 sensu; *Gale* [1996]) and after (couplets C2–C10) the MCE carbon isotope excursion (Figure 6b). Accordingly, the mean $\delta^{13}C$ and $\delta^{18}O$ values of five rhynchonellid and terebratulid genera plot within a narrow range of 2.8 to 3.2‰ and −0.8 to −0.6‰, respectively, whereas the $\delta^{13}C$ and $\delta^{18}O$ values of the terebratulid genera *Kingena*, *Terebratulina* and *Gemmarcula* are depleted by 0.5 to 1.0‰. The isotopic offset for the genus *Gemmarcula* is similar to that observed for the brachiopods in northern Spain. The shells of modern brachiopods contain a high proportion of total organic mass, and terebratulid brachiopods are capable of storing metabolites within extensions of the mantle tissue in their hollow endopunctae [*Curry et al.*, 1989]. It might be possible that genera-dependent incorporation of metabolic CO_2 or early diagenetic alteration due to degradation of organic tissue could have influenced shell carbon isotopic composition of some terebratulid genera. However, high absolute values (~1.0‰ enrichment in comparison to the bulk-carbonate signal for carbon) and low variability in the mean carbon and oxygen isotopic composition of shells from the genera *Orbirhynchia*, *Grasirhynchia*, *Capillithyris*, and *Modestella* argue for a precipitation close to the isotopic

Table 1. Brachiopod-Derived Paleotemperature Estimates for Midlatitude and Subtropical Shelf Seas in Comparison to Temperatures Derived From Paleobotany (Leaf Physiognomy), AGCM, and OGCM Simulations

	$\delta^{18}O_{mean}$, ‰ VPDB	1σ	n	T °C δ_w −1, ‰ SMOW	$\delta_{w,\ low}$, ‰ SMOW	T, °C	$\delta_{w,\ high}$, ‰ SMOW	T, °C	MAT,[a] °C	MASST,[b] °C	MAT,[c] °C CLAMP
Midlatitudes									21–22	18–20	
Late Turonian (without LTE)	−1.90	0.25	83	19–21	−1.5	17–19	−0.5	21–23			
LTE	−1.31	0.29	35	16–18	−1.5	14–16	−0.5	19–21			
Early Turonian	−1.91	0.27	10	19–21	−1.5	17–19	−0.5	21–23			
Late Cenomanian (without CTBE)	−1.14	0.21	11	16–17	−1.5	14–15	−0.5	18–20			
CTBE	−1.67	0.39	27	17–20	−1.5	15–18	−0.5	19–23			
Early-middle Cenomanian (without MCE)	−0.85	0.29	96	15–16	−1.5	12–15	−0.5	16–19			17–20
Mid-Cenomanian (MCE)	−0.60	0.41	25	13–16	−1.5	11–14	−0.5	15–18			
Subtropics, basinal									25–26	22–24	
Late Cenomanian (CTBE)	−1.75	0.42	26	17–21	−0.5	20–23	−0.1	21–25			
Mid-Cenomanian (MCE)	−0.34	0.16	10	13–14	−0.5	15–16	−0.1	16–18			
Subtropics, platform									25–26	22–24	
Middle Turonian	−2.39	0.28	28	21–23	−0.5	23–26	−0.1	25–28			
Late Cenomanian	−2.46	0.38	6	21–24	−0.5	23–26	−0.1	25–28			
Early-middle Cenomanian	−2.58	0.29	34	22–24	−0.5	24–27	−0.1	26–28			

[a]AGCM, GENESIS version 2, 6 × CO_2 simulation [*Flögel*, 2002].
[b]OGCM, POCM, Turonian 4 × CO_2 simulation of *Poulsen et al.* [2001].
[c]Leaf physiognomy of mid-Cenomanian Bohemian floras [*Herman et al.*, 2002].

equilibrium. We cannot exclude the possibility of metabolic effects on the oxygen isotopic composition of Cenomanian-Turonian brachiopods, but estimate the magnitude of these effects <0.5‰ for most of the studied genera. Systematic studies on modern brachiopods are necessary to evaluate taxon-related nonequilibrium isotopic fractionation effects.

5. Results and Discussion

[16] Brachiopods are epifaunal organisms and thrived on the seafloor at shallow water depths. All chalk-sea localities represent a distal shelf environment with water depth between 30 and 100 m, but the occurrence of brachiopods is mostly restricted to the shallower part of sedimentary sequences. Their estimated paleohabitat was in depths between 30 and 50 m. Specimens from northern Spain are associated with shallow water limestones (0–30 m), whereas the localities in the Vocontian basin reflect a deeper environment with an estimated depth range of 30 to 100 m.

[17] Modern articulate brachiopods in temperate regions show slow and continuous shell growth for 8–12 years [*Peck*, 2001]. Assuming a similar age for Cretaceous brachiopods, which usually have sizes between 0.5 and 2 cm, our drilled shell samples most probably reflect an average of several months. Some of the studied brachiopods genera show distinct growth lines, which could reflect seasonal interruptions of shell growth. The relatively small size and the poorer preservation of the anterior shell inhibit an ontogenetic monitoring of shell oxygen isotopic composition within a single specimen, thus we cannot determine the season for which our drilled shell sample is representative. However, seasonality in midlatitude shelf-seas should have an influence on the oxygen isotopic composition of brachiopod shells, and possibly, most of our oxygen isotope values reflect summer conditions. A raw estimation of seasonality could be provided by individuals of the very well preserved Cenomanian species *Orbirhynchia mantelliana*, a species that has no growth lines. The range of $\delta^{18}O$ values in the same interval is about 1‰ (−1.54 to −0.46‰ in couplets B39–40). This quantification is compromised by our uncertainty about possible nonequilibrium isotopic fractionation effects and can not be accepted to be valid for the overall scatter of data, which is probably more related to shell preservation than to seasonality. In order to avoid overinterpretation of single shell data, we applied a nonlinear regression (250 kyr filter) to the composite brachiopod-$\delta^{18}O$ data set (Figure 2). The filtering process averages possible effects of preservation, nonequililibrium precipitation and seasonality, thus we consider the filtered mean $\delta^{18}O$ values (1σ standard deviation) to resemble a mean annual temperature signal, which can be biased somewhat toward summer values (Table 1).

[18] Conservative temperature estimates derived from brachiopod oxygen isotopes were calculated using the equation for shell calcite by [*Anderson and Arthur*, 1983] and a seawater oxygen isotopic composition (δw) of −1‰ SMOW for an ice-free world [*Shackleton and Kennett*, 1975]. Accordingly, mean background chalk-sea temperatures vary between 15 and 16°C in the early middle Cenomanian and display a long-term warming to 16–17°C in the late Cenomanian and to 19–21°C in the early and late Turonian (Figure 2; Table 1). Superimposed on this long-term trend, two periods of decreasing shelf-sea temperatures occurred during the MCE (∼2°C) and the LTE (∼3°C), whereas substantial warming (4–5°C) occurred during the CTBE. In northern Cantabria, mean shelf-sea temperatures range from 22–27°C in the Cenomanian and 20–23°C in the Turonian, whereas in the Vocontian Basin, temperature estimates for the MCE (13–14°C) and the CTBE (18–22°C) are similar to those of midlatitude chalk seas.

[19] The assumption of a temporally and spatially constant δw value is not very reasonable. The validity of our conservative temperature estimates is complicated by the local variability of shelf-sea δw values due to regional

variations in evaporation, precipitation, and runoff, which are difficult to estimate. A prominent facies shift from marly to pure chalk occurred in the late Cenomanian (*guerangeri* zone in NW Germany, uppermost *geslinianum* zone in southern England) in midlatitude shelf sea basins, indicating a diminished terrestrial and fresh-water influx as open oceanic conditions spread [*Hay*, 1995; *Gale et al.*, 2000]. Therefore the effects of increased continental runoff on shelf-sea δw should have been subordinate later than late Cenomanian. In the early to middle Cenomanian, a higher freshwater influx due to increased runoff is a possible scenario. In order to provide a range of possible paleotemperature estimates, two regional δw values are considered as possible end-members for midlatitude localities (Table 1). The lower δw value of −1.5‰ takes into account that continental runoff has effected the oxygen isotopic composition of shelf-seawater, whereas the higher δw value (−0.5‰) considers the effect of the net-precipitation-evaporation balance on surface salinities and seawater δw at paleolatitudes around 35°N [*Zachos et al.*, 1994]. At subtropical shelf localities, evaporation was the main influence on the oxygen isotopic composition of seawater, because of the latitudinal position close to the subtropical high and the reduced terrestrial influx in carbonate platform systems. δw values between −0.5 and −0.1‰ are considered as a reasonable range. Consequently, shelf-sea temperature estimates would increase by 2–3°C at midlatitudes, and by 2–5°C in the subtropics for the case of increased evaporation. In the case of increased continental runoff, midlatitude temperature estimates would be lowered by 2–3°C. The imbalances between sinks and sources for ^{18}O within the hydrological cycle are modeled to result in a −0.2‰ deviation of δw from the present-day value in the Cretaceous [*Wallmann*, 2001]. Accordingly, our estimated temperatures would be lowered by 1–2°C. However, effects of changes in seawater pH on δw underestimate shelf-sea temperatures for higher seawater acidity as a consequence of elevated atmospheric CO_2 levels and would, therefore, increase our temperatures estimates by 2–3.5°C [*Zeebe*, 2001].

[20] Several independent paleotemperature estimates derived from climate and ocean modeling and paleobotany can be compared with the different scenarios for $\delta^{18}O$-derived temperatures (Table 1). Results of a Cenomanian-Turonian Earth system model with 6 × atmospheric CO_2 (GENESIS, version 2.0) predict mean annual temperatures of 21–22°C for 35°N, and 25–26°C for 27°N [*Flögel*, 2002]. According to the results of a Turonian ocean circulation model (OGCM) with 4 times atmospheric CO_2 (parallel ocean climate model (POCM)), mean SSTs are between 18–20°C at midlatitudes and 22–24°C in the subtropics [*Poulsen et al.*, 2001]. Analysis of the leaf physiognomy of mid-Cenomanian flora from Bohemia using the CLAMP technique shows mean annual temperatures between 17 and 20°C for the mid-European Island (~33°N) [*Herman et al.*, 2002].

[21] In the Cenomanian, model-predicted and floral-derived temperatures agree best with midlatitude $\delta^{18}O$-derived temperatures, which use a higher δw value for effects of increased evaporation. The assumption of a reduced δw value due to enhanced continental runoff results in relatively low temperatures, which underestimate ocean-model-predicted temperatures by 3–5°C. In the Turonian, the best agreement between $\delta^{18}O$- and model-derived temperatures is obtained for the scenario with low δw values. A shift from evaporation-dominated to runoff dominated seawater oxygen isotopic composition would explain much of the observed long-term Cenomanian-Turonian $\delta^{18}O$ decrease in brachiopod shell calcite. However, such a temporal trend is opposite to the observed facies change from marly to pure chalk, which indicates a reduction of terrestrial and freshwater influx in the Turonian. We, therefore, assume that the long-term decrease in brachiopod $\delta^{18}O$ values is probably related more to temperature than to changes in the oxygen isotopic composition of seawater. The estimated temperature rise of 6°C for stable δw values in the Cenomanian-Turonian would be amplified if a reduction of continental runoff (increase of δw) is taken into account, and thus represents a conservative minimum estimate.

[22] At subtropical localities in northern Spain, the lower δw estimate (−0.5‰) shows the best agreement to model-predicted temperatures, whereas in southern France, the lower δw estimate results in temperatures, which underestimate model temperatures by 2–7°C. The relatively low temperature estimates are explained by the deeper depth habitat of brachiopods in the Vocontian Basin.

6. Paleoclimatic and Paleoceanographic Implications

[23] The middle to early late Cenomanian part of our two brachiopod shelf-sea temperature records supplement $\delta^{18}O$-derived temperatures of tropical, subtropical and temperate oceanic surface, thermocline and deeper waters (Sites 144, 1050, 551) [*Huber et al.*, 2002; *Norris et al.*, 2002; *Gustafsson et al.*, 2003], forming a transect across the central northern Atlantic ocean from the tropics to the midlatitudes (Figure 1). The mean oxygen isotopic composition of calcitic shells at each locality in combination with modeled salinities [*Poulsen et al.*, 2001] allow the estimation of possible salinity-temperature ranges for different water masses, thus providing a latitudinal salinity-temperature-density profile (Table 2; Figure 7). In order to provide a reasonable paleotemperature range for each locality and water depth, a range of regional δw values is taken into account (Table 2). Surface water δw values at midlatitudes (European shelf sea and Site 551, Goban Spur) and at subtropical localities (northern Spain and Site 1050, Blake Nose) are considered within the ranges discussed above. The tropical surface water δw range is discussed by *Norris et al.* [2002], where the authors used the present-day range of δw values at Demerara rise corrected for an ice-free world. In the deeper ocean (intermediate to deep waters), the conservative δw value of −1.0 0.2 l SMOW for an ice-free world is a reasonable estimate. Paleotemperature ranges are calculated by using the equations of *Anderson and Arthur* [1983] for brachiopods, of *Bemis et al.* [1998] for non-symbiontic planktic foraminifera and of *Shackleton* [1974] for benthic foraminifera. Application of these different paleotemperature equations implies an error of ~1°C, but considers differences in biogenic calcite precipitation.

Table 2. Ranges of Calcite $\delta^{18}O$ Values, Estimated δw Values and Temperatures, and Modeled Salinities at Different Localities in the Late Cenomanian Proto-North Atlantic Ocean

Locality	Latitude, °N	Depth, m	Stratigraphy	Fossil	$\delta^{18}O_c$,[a] ‰ V-PDB	n	δ_w,[b] ‰ SMOW	$T_{calculated}$,[c] °C	$S_{modeled}$,[d] psu	$T_{modeled}$,[d] °C
NW Europe	35–36	30–50	*acutus-guerangeri*	brachiopods	−1.4 to −0.9	24	−1.2 to −0.5	15–20	33–35[h]	14–20
N Spain	25–27	20–50	*rhotomagense*	brachiopods	−2.7 to −2.2	18	−0.5 to −0.1	23–28	35–35.5	22–24
Site 1050[e]	25	mixed layer	*cushmani*	planktic foraminifera	−2.6 to −1.9	10	−0.5 to −0.1	23–28	35.5–36.5	24–26
Site 1050	25	thermocline	*cushmani*	*Rotalipora* ssp	−1.7 to −1.4	6	−0.4 to −0.2	21–24	35.5–36.0	-
Site 1050	25	∼1500	*cushmani*	benthic foraminifera	−1.1 to −0.6	6	−1.2 to −0.8	14–18	35.3–35.7	15–16
Site 551[f]	35–36	mixed layer	*cushmani*	*H. delrioensis*	−2.0 to −1.6	6	−1.2 to −0.5	18–24	34–35	16–18
Site 551	35–36	thermocline	*cushmani*	*R. greenhornensis*	−1.8 to −1.6	6	−1.0 to −0.7	19–22	34–35	-
Site 551	35–36	∼2500	*cushmani*	*G. lenticulus*	−0.8 to −0.6	11	−1.2 to −0.8	15–17	35.3–35.7	15–16
Site 144[g]	5	mixed layer	IC 49/50	*H. delrioensis*	−4.1 to −3.8	20	−0.6 to 0.2	32–37	35–35.5	30–32

[a]The $\delta^{18}O_c$ range refers to the mean oxygen isotopic composition of well-preserved fossil calcite ± 1σ standard deviation.
[b]Estimated regional δw ranges (see text for discussion).
[c]Calculated temperature range include variations in both $\delta^{18}O_c$ and δ_w.
[d]OGCM salinities and temperatures modeled by the Turonian 4 × CO_2 and Albian 4 × CO_2 simulations for surface and deeper waters [*Poulsen et al.*, 2001].
[e]The $\delta^{18}O$ data of *Huber et al.* [2002].
[f]The $\delta^{18}O$ data of *Gustafsson et al.* [2003].
[g]The $\delta^{18}O$ data of *Norris et al.* [2002].
[h]Intermediate range between Tethyan high and boreal low salinity waters (see text).

Regional surface water salinities, predicted by Albian and Turonian ocean circulation simulations (POCM) [*Poulsen et al.*, 2001], are attributed to the calculated temperature ranges. The Turonian simulation of *Poulsen et al.* [2001] provides the best scenario for surface waters exchange across shallow seas after the Cenomanian first-order sea level rise. The Cenomanian deeper proto-North Atlantic probably had no deep-water exchange with the Southern Ocean [*Summerhayes*, 1987; *Pletsch et al.*, 2001], thus calculated temperature ranges of deeper water masses are assigned to model-predicted salinities of the Albian simulation, which consider the North Atlantic ocean as an isolated basin. Model-predicted surface water salinities at midlatitude shelf seas cover a broad range from low boreal (28 psu) to high Tethyan (36 psu) salinities [*Poulsen et al.*, 2001]. The low boreal model salinities result from geographic isolation of boreal seas as a consequence of low-resolution paleogeography. We, therefore, used an intermediate range of 32–35 psu for the European shelf-sea, in order to account for the open exchange of surface waters between the Boreal and Tethyan seas in the Cenomanian-Turonian, which is evident from the geological record but not resolved by the ocean model. In order to test the validity of our approach of relating $\delta^{18}O$-derived temperatures to modeled salinities, we examined the agreement of $\delta^{18}O$-derived and ocean model-predicted temperatures (Table 2). The $\delta^{18}O$-derived temperatures match very well for intermediate to deep waters and midlatitude shelf-seawaters. For tropical to subtropical surface and subtropical to temperate shelf-seawaters, the lower value of the estimated $\delta^{18}O$-derived temperatures range agrees with model-predicted temperatures.

[24] The corresponding temperature-salinity pairs of variables for each water mass describe distinct arrays within the salinity-temperature-density diagram [*Millero and Poisson*, 1981] (Figure 7). Surface waters with the lowest density occurred in the tropics (Site 144), where sea-surface temperatures were extraordinarily warm and salinities were partly influenced by the Intertropical Convergence Zone (see discussion in the work of *Wilson et al.* [2002]). Toward the subtropics (Site 1050 and northern Spain), surface water density increased as a consequence of increasing salinity and decreasing temperature beneath the subtropical high and within the subtropical gyre. At midlatitudes, temperate surface and shelf-seawaters (Site 551 and European shelf sea) cover a broad array of possible temperature-salinity ranges due to uncertainties about the regional effects of continental runoff. In the case of lower surface salinity (lower δw estimate due to enhanced runoff and/or precipitation), corresponding temperatures are relatively low (15–19°C), and the density resembles that of the warmer and more saline subtropical surface waters. In the case of higher salinities and temperatures (higher δw estimate), the temperate surface water at Goban Spur and the European shelf-seas form the highest density surface water in the Cenomanian proto-North Atlantic ocean (Figure 7). The oxygen isotopic composition of benthic foraminifera at Site 1050 [*Huber et al.*, 20002] and Site 551 [*Gustafsson et al.*, 2003] is similar at both sites and reflects the conditions of intermediate to deep waters at 1500 to 2500 m water depth. The estimated temperature range is 15–18°C at both localities.

[25] Results of ocean and coupled atmosphere-ocean simulations for the Campanian and Cenomanian-Turonian indicate that oceanic deep waters can be formed by cooling warm and salty water in the high latitudes of the northern Pacific and southern hemisphere [*Brady et al.*, 1998; *Poulsen et al.*, 2001; *Bice and Norris*, 2002], which is contrary to the older theory of warm saline deep water formation at low latitudes [*Brass et al.*, 1982]. During the Cenomanian, the North Atlantic ocean was an isolated basin with either no or only limited global deep water exchange. Deep water connections toward the Arctic ocean were blocked until the opening of the Greenland-Iceland-Norwegian Sea in the Oligocene [*Wold*, 1995]. The isthmus between North and South America was only open to depths of 400–700 m

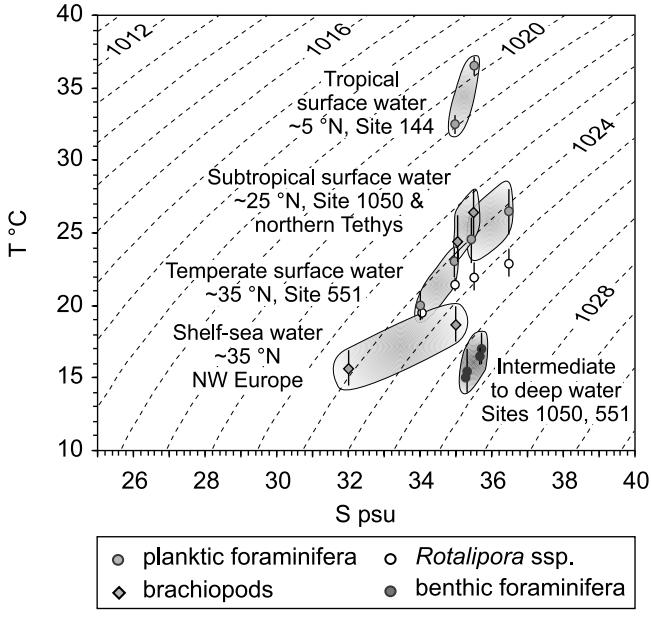

Figure 7. Salinity-temperature-density diagram of *Millero and Poisson* [1981] showing late Cenomanian North Atlantic water mass arrays based on δ^{18}O-derived temperature estimates of planktic and benthic foraminifera and brachiopods and modeled regional salinities from the Turonian (surface waters) and Albian (deeper waters) 4 × CO_2 POCM simulations of *Poulsen et al.* [1999] (see text and Table 2). The diagram is the graphical representation of the equation of state for seawater at the sea surface. Dashed lines represent densities of water at the surface in kg m^{-3}. Temperature ranges for surface, thermocline, and intermediate to deep waters are calculated by using the mean oxygen isotopic composition of shell calcite within the error of 1σ standard deviation, and δw values, which consider (1) an ice volume correction (δw = −1‰ SMOW) for an ice-free earth and (2) an estimated regional range that takes account of paleolatitude, possible runoff, and evaporation. The calculated temperature ranges for the lower δw value at each locality are assigned to the lower modeled regional salinity. Data are from this study, *Norris et al.* [2002], *Huber et al.* [2002], and *Gustafsson et al.* [2003]. Surface waters with highest densities occurred at midlatitude epicontinental seas, if continental runoff is low, and could have been a possible source of Cenomanian North Atlantic intermediate to deep water.

[*Otto-Bliesner et al.*, 2002], and toward Tethys, deep water connections were inhibited or restricted by the continental terranes of Apulia and the Taurides [*Dercourt et al.*, 1992]. The deep gateway between the North and South Atlantic oceans is supposed to have opened in the latest Cenomanian to early Turonian [*Pletsch et al.*, 2001]. Hence during most of the Cenomanian time, proto-North Atlantic deep waters originated from a regional source. The oxygen isotopic composition of midlatitude brachiopods, which reflect mean annual or summer conditions, is very similar to those of benthic foraminifera at sites 1050 and 551. The temperate shelf-seawaters of northwestern Europe had the highest surface water density, if higher rates of evaporation and low continental runoff (higher δw estimate) are assumed, which describes a situation similar to the Mediterranean Sea today. The density of temperate surface waters would be even higher, if the range of brachiopod-δ^{18}O values during a certain time interval is a measure of seasonality, as discussed for the middle Cenomanian species *O. mantelliana* (see above), and the higher δ^{18}O value (−0.5‰) would reflect winter conditions. We, therefore speculate, that the dense temperate shelf-seawater could have contributed either seasonally (during winter times) or episodically to intermediate and/or deeper waters in the Cenomanian isolated proto-North Atlantic basin. This idea is supported by a north-south gradient in preservation of organic matter. Highest rates of organic carbon accumulation occurred at the southern edge of the North Atlantic basin (DSDP Sites 144, 367, Tarfaya Basin) [*Kuhnt et al.*, 1990; *Kuypers et al.*, 2002], indicating the occurrence of the oldest and less oxygenated deep waters there.

[26] Shelf-sea temperatures varied considerably during the Cenomanian-Turonian time interval, revealing changes in the order of 100 kyr during the three carbon cycle events MCE, CTBE and LTE (Figures 2 and 8). The minor δ^{13}C events, MCE and LTE, have similar temperature trends, showing an initial cooling (2–3°C) that peaks close to the δ^{13}C maximum, and a subsequent warming interval. This overall trend is closely related to large-amplitude sea level changes indicated by incision, condensation, lowstand sediments and subsequent transgressive sequences at shallow shelf settings.

[27] The commencement of the MCE-δ^{13}C excursion falls in the *C. inerme* ammonite zone, which was regressive on a global scale (India, Boreal and Tethyan European Basins, New Jersey margin) [*Gale et al.*, 2002; *Miller et al.*, 2003; *Wilmsen*, 2003]. The subsequent transgression coincides with the δ^{13}C maximum and is related to the basal *A. rhotomagense* ammonite zone. The sudden increase of Sr concentrations in brachiopod shells is also of *C. inerme* zone age (Figure 4). The large magnitude of changes in the Sr concentration exceeds any variability, which is known from modern calcite precipitating organisms due to the influence of changes in seawater temperature or rates of growth and calcification [e.g., *Lea et al.*, 1999]. The most probable explanation for the fast and large strontium increase is a variation in the Sr/Ca ratio of seawater as a consequence of the rapid, short-term regression [*Stoll and Schrag*, 1998; *Stoll and Schrag*, 2001]. The large amount of Sr is recycled to seawater during subaerial exposure and meteoric diagenesis of previously deposited shallow water carbonates, which were dominated by aragonitic communities in the Albian-Cenomanian time [*Stanley and Hardie*, 1998; *Steuber and Veizer*, 2002].

[28] In western Europe, the southward spread of boreal invertebrates (bivalves, belemnites) indicates the occurrence of two MCE cooling pulses, the first related to the initial δ^{13}C bulk-carbonate increase (*arlesiensis* bed) and the second to the δ^{13}C maximum (*primus* bed; Figure 8a) [*Paul*

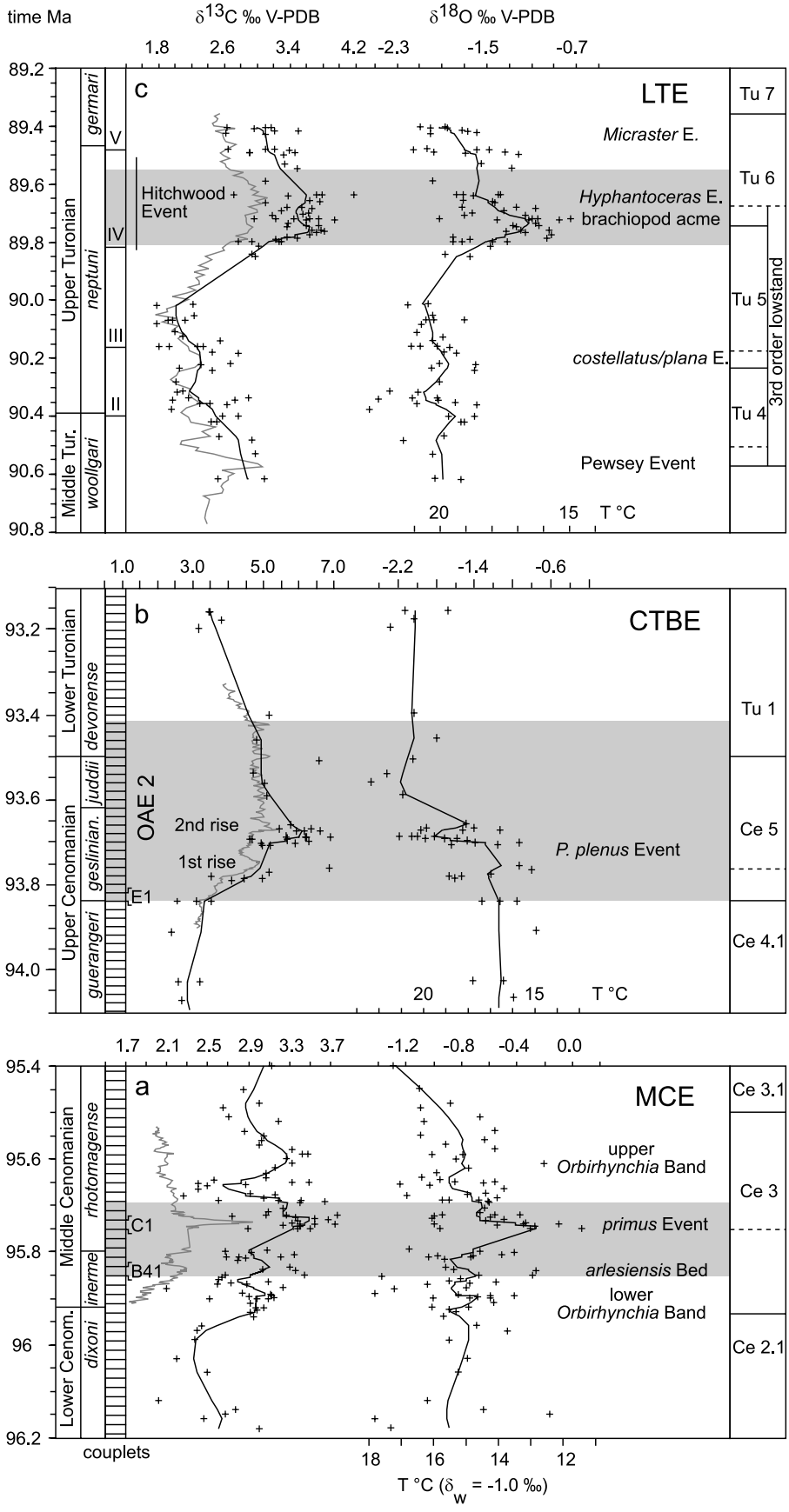
time Ma
δ13C ‰ V-PDB
δ18O ‰ V-PDB
1.8 2.6 3.4 4.2 -2.3 -1.5 -0.7
c
LTE
Micraster E.
Hitchwood Event
Hyphantoceras E.
brachiopod acme
costellatus/plana E.
Pewsey Event
20 15 T °C
Upper Turonian
Middle Tur.
germari
neptuni
woollgari
V
IV
III
II
Tu 7
Tu 6
Tu 5
Tu 4
3rd order lowstand
1.0 3.0 5.0 7.0 -2.2 -1.4 -0.6
b
CTBE
OAE 2
2nd rise
1st rise
E1
P. plenus Event
20 15 T °C
Lower Turonian
Upper Cenomanian
devonense
juddii
geslinian.
guerangeri
Tu 1
Ce 5
Ce 4.1
1.7 2.1 2.5 2.9 3.3 3.7 -1.2 -0.8 -0.4 0.0
a
MCE
upper Orbirhynchia Band
C1
primus Event
B41
arlesiensis Bed
lower Orbirhynchia Band
Middle Cenomanian
Lower Cenom.
rhotomagense
inerme
dixoni
Ce 3.1
Ce 3
Ce 2.1
couplets
18 16 14 12
T °C (δw = -1.0 ‰)
89.2 89.4 89.6 89.8 90.0 90.2 90.4 90.6 90.8
93.2 93.4 93.6 93.8 94.0
95.4 95.6 95.8 96 96.2

Figure 8

et al., 1994]. Both bioevents are sandwiched between a lower and an upper *Orbirhynchia* event forming a bundle of bioevents across the lower-middle Cenomanian transition. $\delta^{18}O$-derived shelf-sea temperatures indicate that the temperature minimum corresponds to the occurrence of the boreal belemnite *Praeactinocamax primus*. The main temperature decrease correlates with the sea level lowstand and is followed by subsequent warming during transgression. The overall duration of the MCE is about 200 kyr.

[29] Cenomanian carbon isotopic data from benthic and planktonic foraminifera at Site 1050 show a distinct positive excursion, thus providing the first evidence for the presence of the MCE in a deep-sea section [*Huber et al.*, 2002] (Figure 2). During the MCE, thermocline and deep water temperatures decrease by ~3°C, thus showing the same trend as our midlatitude shelf-sea temperatures. Overall cooling in deeper, thermocline and shelf waters indicates a general change in North Atlantic ocean circulation that probably favored increased oceanic ventilation and upwelling of nutrient-rich water masses, and could drive the positive carbon isotope excursion.

[30] The relation between eustasy and the LTE is more difficult to reconstruct due to the lack of overregional correlations of sedimentary sequences. Biostratigraphically, the LTE is placed in the mid-*S. neptuni* ammonite zone of the European zonation and refers to the *Scaphites nigricollensis* to *Prionocyclus quadratus* ammonite zones in North America [*Walaszczyk and Cobban*, 2000], and to the *Inoceramus costellatus* and *I. inaequivalvis* inoceramid zones in Russia and northern Siberia [*Zakharov et al.*, 1991; *Sahagian et al.*, 1994]. In western Europe, the LTE is characterized by a distinct cooling trend (3–4°C) associated with a positive $\delta^{13}C$ excursion (Figure 8c) [*Voigt*, 2000; *Voigt and Wiese*, 2000]. According to the age model, the duration for the LTE can be estimated to be in the order of 200 to 400 kyr. A major late Turonian third-order sea level drop is indicated by the Exxon sea level curve [*Hardenbol et al.*, 1998] (Figure 8a). This large regression lasted about 1 million years, caused a widespread hiatus in the Western Interior Basin [*Cobban and Scott*, 1972; *Leckie et al.*, 1997; *Sageman et al.*, 1997], in western Europe [e.g., *Hancock*, 1989] on the Russian Platform and in northern Siberia [*Sahagian and Jones*, 1993; *Sahagian et al.*, 1994]. The LTE has so far only been recorded from different European basinal sections, where several sedimentary sequences are superimposed on the late Turonian long-term sea level fall and rise (Figure 8c) [*Wiese et al.*, 2004]. The occurrence of temporal expanded stratigraphical gaps at marginal settings and the lack of $\delta^{13}C$ stratigraphies from other continental cratons have inhibited so far a precise correlation of high-order sequences with eustatic sea level changes. However, the late third-order sea level lowstand can be correlated with the initial LTE-$\delta^{13}C$ increase. The subsequent transgression caused the development of sedimentary onlap surfaces in all basins of western Europe, North America, Russia and northern Siberia, and corresponds to the interval yielding the $\delta^{13}C$ decrease in the *Prionocyclus germari* ammonite zone. The decrease of shelf-sea temperatures during the LTE refers only to a short interval of the global sea level lowstand and represents one of the European fourth-order sequences (Tu 6 in Figure 8a) [*Wiese et al.*, 2004]. The subsequent rise of shelf-sea temperatures corresponds to the third-order transgression.

[31] At a first glance, our observed shelf-sea temperature variations correlate with falling and rising sea level during the MCE and LTE. The amplitude of the eustatic sea level change is larger than 10 m (20–30 m) in both cases, and the duration of the $\delta^{13}C$ event approaches frequencies of orbital forcing. Thus our data would support the hypothesis of short-term growth of glaciers as a glacioeustatic mechanism for fast and high-amplitude sea level changes during greenhouse climate conditions [*Miller et al.*, 2003]. However, the linkage between sea level and temperature is not straightforward in the shelf-sea settings. During the MCE, the coolest temperature estimate is related to the bed identified as a transgressive surface. During the LTE, the cooling of shelf-sea temperatures occurred only within a short interval during the major third-order sea level lowstand. If there was a linkage between waxing and waning of polar ice and sea level, the cooling of shelf-sea temperatures underwent probably not a direct forcing. Regional changes of shelf-sea circulation as a consequence of changes in sea level and North Atlantic circulation are a more realistic mechanism to explain the observed shelf-sea temperature variation.

[32] Shelf-sea temperature evolution throughout the CTBE shows a prominent increase of about 4°C during the late $\delta^{13}C$ excursion, when a second $\delta^{13}C$ increase in the inorganic carbon reservoir occurred (~150 kyr after initiation of OAE 2, Figure 8b). The temperature rise is preceded by a brief cooling interval (10–20 kyr duration), which is not resolved by our $\delta^{18}O$ record, but evident from the southward spread of boreal taxa [*Jefferies*, 1962; *Gale and Christensen*, 1996]. The short cool-pulse in the middle of OAE 2 occurred shortly after the main $\delta^{13}C$ excursion (10–20 kyr), and can be seen as a first climate feedback related to increased rates of global organic carbon burial and reduction of atmospheric CO_2 [*Arthur et al.*, 1987; *Kuypers et al.*, 1999]. Instead, the late and longer warming trend

Figure 8. Brachiopod derived $\delta^{13}C$ and $\delta^{18}O$ variations during the carbon isotope events (a) MCE, (b) CTBE, and (c) LTE in the temperate shelf sea of western Europe. In order to demonstrate temporal changes, isotopic data are smoothed with an (a) 130 kyr, (b) 400 kyr, and (c) 200 kyr filter, respectively. Light gray shaded intervals mark the $\delta^{13}C$ events. Dark gray $\delta^{13}C$ curves are bulk-rock curves of the sections Salzgitter-Salder (Figure 8c) [*Voigt and Hilbrecht*, 1997], Eastbourne (Figure 8b) [*Paul et al.*, 1999], and Folkestone (Figure 8a) [*Paul et al.*, 1994]. Roman numerals indicate (Figure 8c) bentonites (see Figure 2) and (Figures 8a and 8b) sedimentary couplets, which reflect precessional rhythms [*Gale et al.*, 1999]. Fourth-order sedimentary sequences are from the work of *Gale et al.* [2002] in the Cenomanian and *Wiese et al.* [2004] in the late Turonian.

seems more to be related to the causes of the second $\delta^{13}C$ rise and ongoing carbon cycle perturbation. Increased rates of volcanism and hydrothermal activity, as a consequence of the emplacement of large oceanic plateau basalts, were suggested as the cause of increased greenhouse gas forcing and enhanced nutrient availability, considered to be crucial for both the initiation and the response of the Cenomanian-Turonian carbon cycle perturbation [*Larson*, 1991; *Orth et al.*, 1993; *Sinton and Duncan*, 1997; *Kerr*, 1998]. An additionally proposed mechanism for OAE 2 is the opening of a deep water connection between the North and South Atlantic oceans [*Tucholke and Vogt*, 1979; *Summerhayes*, 1987; *Pletsch et al.*, 2001; *Kuypers et al.*, 2002]. *Poulsen et al.* [2003] performed coupled atmosphere-ocean model simulations to study the climatic effect of gateway opening, and found substantial oceanographic changes in their post-rifting experiment. Accordingly, North Atlantic surface waters experienced both freshening (0.5–1‰) and warming (0.5°C), which would partly account for the observed 1.0‰ $\delta^{18}O$ decrease in brachiopod calcite. A substantial change in ocean and shelf-sea circulation is also indicated by the spread of oligotrophic conditions in western European shelf seas in relation to the sea level rise contemporaneous with the second $\delta^{13}C$ rise [*Gale et al.*, 2000]. A further implication of warming and freshening of European shelf-seawater would be the lowering of its density, which could have forced a cessation of deep water formation. Interesting in this context is, that the evidence of photic zone anoxia in the southern North Atlantic ocean is also related to the late OAE 2 carbon isotope excursion [*Kuypers et al.*, 2002], supporting the idea of a diminished or collapsed oceanic ventilation within the North Atlantic as a late feedback. On the other side, enhanced production of deepwater on shelves, which drives oceanic overturn, productivity, and the positive $\delta^{13}C$ excursion is a long-time proposed mechanism for OAE 2 [*Arthur et al.*, 1988]. Here we can only speculate that increased oceanic overturn and ventilation were probably related to the early phase of OAE 2. Oceanic surface-to-deep water temperature gradients with a sufficient temporal resolution are needed to address the question whether diminished and/or enhanced oceanic circulation are accompanied with the Cenomanian-Turonian carbon cycle perturbation.

7. Conclusions

[33] An 8 million year midlatitude $\delta^{18}O$-derived shelf-sea temperature record, based on well-preserved brachiopod shells, reveals a long-term climate warming through the Cenomanian that reached a maximum (23°C) in the early to early late Turonian. The most prominent temperature rise of 4–5°C occurred during the CTBE, indicating a major turnover of thermohaline circulation in the North Atlantic basin. A comparison of open oceanic and shelf sea $\delta^{18}O$ data from tropical and subtropical sites with those from the temperate midlatitudes demonstrates the opportunity that the temperate shelf-seawaters could have had the highest density surface waters in the Cenomanian North Atlantic ocean if the continental runoff was low. Owing to the restriction of deep water connections by geographic barriers, waters of the temperate to boreal shelf seas could have contributed to the formation of intermediate and/or deeper waters. Two minor shelf sea cooling events in the mid-Cenomanian and late Turonian coincide with carbon cycle perturbations and large amplitude sea level falls, and thus provide supporting evidence for potential glacioeustatic effects. However, the linkage between sea level and temperature is not straightforward in shelf-sea settings. During the MCE, the temperature minimum correlates with a transgressive bed, and during the LTE, shelf-sea cooling represents only a brief interval within the major third-order sea level lowstand. Regional changes in shelf-sea circulation as a consequence of changes in sea level and North Atlantic circulation are the most plausible mechanism to explain the observed shelf-sea temperature variations.

[34] **Acknowledgments.** We thank Frank Wiese, Markus Wilmsen and Rory Mortimore for providing brachiopod samples and assistance during field work. The insightful reviews by Karen Bice, Paul Wilson and Mike Arthur are gratefully acknowledged. Kay Stone is thanked for her grammatical corrections. This work was supported by grants of the Deutsche Forschungsgemeinschaft (VO 387/3 and Ha 2891/3).

References

Anderson, T. F., and M. A. Arthur (1983), Stable isotopes of oxygen and carbon and their application to sedimentologic and palaeoenvironmental problems, *Soc. Econ. Palaeontol. Mineral. Short Course*, *10*, I.1–I.151.

Arthur, M. A., S. O. Schlanger, and H. C. Jenkyns (1987), The Cenomanian-Turonian oceanic anoxic event, II. Palaeoceanographic controls on organic matter production and preservation, *Geol. Soc. Spec. Publ.*, *26*, 401–420.

Arthur, M. A., W. E. Dean, and L. M. Pratt (1988), Geochemical and climatic effects of increased marine organic carbon burial at the Cenomanian/Turonian boundary, *Nature*, *335*, 714–717.

Auclair, A.-C., M. M. Joachimski, and C. Lécuyer (2003), Deciphering kinetic, metabolic and environmental controls on stable isotope fractionations between seawater and the shell of *Terebratalia transversa* (Brachiopoda), *Chem. Geol.*, *202*, 59–78.

Bemis, B. E., H. Spero, J. Bijma, and D. W. Lea (1998), Reevaluation of the oxygen isotopic composition of planktonic foraminifera: Experimental results and revised paleotemperature equations, *Paleoceanography*, *13*, 150–160.

Bice, K. L., and R. D. Norris (2002), Possible atmospheric CO_2 extremes of the Middle Cretaceous (late Albian–Turonian), *Paleoceanography*, *17*(4), 1070, doi:10.1029/2002PA000778.

Bice, K. L., B. T. Huber, and R. D. Norris (2003), Extreme polar warmth during the Cretaceous greenhouse? Paradox of the late Turonian $\delta^{18}O$ record at Deep Sea Drilling Project Site 511, *Paleoceanography*, *18*(2), 1031, doi:10.1029/2002PA000848.

Brady, E. C., R. M. DeConto, and S. L. Thompson (1998), Deep water formation and poleward ocean heat transport in the warm climate extreme of the Cretaceous (80 Ma), *Geophys. Res. Lett.*, *25*, 4205–4208.

Brand, U., and P. Brenckle (2001), Chemostratigraphy of the mid-Carboniderous boundary global stratotype and point (GSSP), Bird Spring Formation, Arrow Canyon, Nevada, USA, *Palaeogeogr. Palaeoclimatol. Palaeoecol.*, *165*, 321–347.

Brand, U., A. Logan, N. Hiller, and J. Richardson (2003), Geochemistry of modern brachiopods: Application and implication for oceanography and paleoceanography, *Chem. Geol.*, *198*, 305–334.

Brass, G. W., J. R. Southam, and W. H. Peterson (1982), Warm saline bottom waters in the ancient ocean, *Nature*, *296*, 620–623.

Buening, N., and H. J. Spero (1996), Oxygen and carbon isotope analyses of the articulate brachiopod *Laqueus californianus*: A recorder of environmental changes in the subeuphotic zone, *Mar. Biol.*, *127*, 105–114.

Carpenter, S. J., and K. C. Lohmann (1995), $\delta^{18}O$ and $\delta^{13}C$ values of modern brachiopod shells, *Geochim. Cosmochim. Acta*, *59*, 3749–3764.

Clarke, L. J., and H. C. Jenkyns (1999), New oxygen-isotope evidence for long-term Cretaceous climate change in the Southern Hemisphere, *Geology*, *27*, 699–702.

Cobban, W. A., and G. R. Scott (1972), Stratigraphy and ammonite fauna of the Graneros Shale and Greenhorn Limestone near Pueblo, Colorado, *U.S. Geol. Surv. Prof. Pap.*, *645*, 1–108.

Curry, G. B., and A. E. Fallick (2002), Use of stable oxygen isotope determinations from brachiopod shells in palaeoenvironmental reconstruction, *Palaeogeogr. Palaeoclimatol. Palaeoecol.*, *182*, 133–143.

Curry, G. B., A. D. Ansell, M. James, and L. Peck (1989), Physiological constraints on living and fossil brachiopods, *Trans. R. Soc. Edinburgh Earth Sci.*, *80*, 255–262.

Dercourt, J., L. E. Ricou, and B. Vrielynck (1992), *Atlas Tethys*, Paleoenviron. Maps, Paris.

Erbacher, J., J. Thurow, and R. Littke (1996), Evolution patterns of radiolaria and organic matter variations: A new approach to identify sea-level changes in mid-Cretaceous pelagic environments, *Geology*, *24*, 499–502.

Flögel, S. (2002), On the influence of precessional Milankovitch cycles on the late Cretaceous climate system: Comparison of GCM results, geochemical, and sedimentary proxies for the western interior seaway of North America, Ph.D. thesis, Univ. of Kiel, Kiel, Germany.

Gale, A. S. (1996), Turonian correlation and sequence stratigraphy of the Chalk in southern England, *Geol. Soc. Spec. Publ.*, *103*, 177–195.

Gale, A. S., and W. K. Christensen (1996), Occurrence of the belemnite *Actinocamax plenus* in the Cenomanian of SE France and its significance, *Bull. Geol. Soc. Denmark*, *43*, 68–77.

Gale, A. S., J. R. Young, N. J. Shackleton, S. J. Crowthurst, and D. S. Wray (1999), Orbital tuning of Cenomanian marly chalk successions: Towards a Milankovitch time-scale for the late Cretaceous, *Philos. Trans. R. Soc. London A*, *357*, 1815–1829.

Gale, A. S., A. B. Smith, N. E. A. Monks, J. A. Young, A. Howard, D. S. Wray, and J. M. Huggett (2000), Marine biodiversity through the late Cenomanian-early Turonian: Palaeoceanographic controls and sequence stratigraphic biases, *J. Geol. Soc.*, *157*, 745–757.

Gale, A. S., J. Hardenbol, B. Hathway, J. W. Kennedy, J. R. Young, and V. Phanskalar (2002), Global correlation of Cenomanian (upper Cretaceous) sequences: Evidence for Milankovitch control on sea level, *Geology*, *30*, 291–294.

Gradstein, F. M., F. P. Agterberg, J. G. Ogg, J. Hardenbol, P. Van Veen, J. Thierry, and Z. Huang (1995), A Triassic, Jurassic and Cretaceous time scale, in *Geochronology, Time Scales and Global Stratigraphic Correlation*, *Soc. Econ. Palaeontol. Mineral. Spec. Publ.*, vol. 54, edited by W. A. Berggren et al., pp. 95–126, Soc. for Sediment. Geol., Tulsa, Okla.

Gustafsson, M., A. Holbourn, and W. Kuhnt (2003), Changes in northeast Atlantic temperature and carbon flux during the Cenomanian/Turonian paleoceanographic event: The Gobal Spur stable isotope record, *Palaeogeogr. Palaeoclimatol. Palaeoecol.*, *201*, 51–66.

Hancock, J. M. (1989), Sea-level changes in the British region during the Cretaceous, *Proc. Geol. Assoc.*, *100*, 565–594.

Hardenbol, J., J. Thierry, M. B. Farley, T. Jaquin, P.-C. Graciansky, and P. Vail (1998), Mesozoic and Cenozoic sequence chronostratigraphic framework of European basins, in *Mesozoic and Cenozic Sequence Stratigraphy of European Basins*, *Soc. Econ. Palaeontol. Mineral. Spec. Publ.*, vol. 60, edited by P.-C. Graciansky et al., pp. 3–13, Soc. for Sediment. Geol., Tulsa, Okla.

Hay, W. W. (1995), A comparison of modern and Cretaceous paleoceanography, *Geol. Carpathica*, *46*, 257–266.

Herman, A. B., R. A. Spicer, and J. Kvacek (2002), Late Cretaceous climate of Eurasia and Alaska: A quantitative approach, in *Aspects of Cretaceous Stratigraphy and Palaeobiogeography*, *Schr. Erdwissensch. Komm.*, vol. 15, edited by M. Wagreich, pp. 93–108, Austrian Acad. of Sci., Vienna.

Huber, B. T., R. M. Leckie, R. D. Norris, T. J. Brawlower, and E. CoBabe (1999), Foraminiferal assemblage and stable isotopic change across the Cenomanian-Turonian boundary in the subtropical North Atlantic, *J. Foraminiferal Res.*, *29*, 392–417.

Huber, B. T., R. D. Norris, and K. G. MacLeod (2002), Deep-sea paleotemperature record of extreme warmth during the Cretaceous, *Geology*, *30*, 123–126.

James, N. P., Y. Bone, and T. K. Kyser (1997), Brachiopod $\delta^{18}O$ values do reflect ambient oceanography: Lacepede Shelf, southern Australia, *Geology*, *25*, 551–554.

Jefferies, R. P. S. (1962), The palaeoecology of the *Actinocamax plenus* subzone (lowest Turonian) in the Anglo-Paris basin, *Palaeontology*, *4*, 609–647.

Kerr, A. C. (1998), Oceanic plateau formation: A cause of mass extinction and black shale deposition around the Cenomanian-Turonian boundary?, *J. Geol. Soc.*, *155*, 619–626.

Klein, R. T., K. C. Lohmann, and C. W. Thayer (1996), Sr/Ca and 13C/12C ratios in skeletal calcite of *Mytilus trossulus*: Covariation with metabolic rate, salinity, and carbon isotopic composition of seawater, *Geochim. Cosmochim. Acta*, *60*, 4207–4221.

Kuhnt, W., J. Thurow, J. Wiedmann, and J. P. Herbin (1986), Oceanic anoxic conditions around the Cenomanian/Turonian boundary and the response of the biota, *Mitt. Geol. Paläontol. Inst. Univ. Hamburg*, *60*, 205–246.

Kuhnt, W., J. P. Herbin, J. Thurow, and J. Wiedmann (1990), Distribution of Cenomanian-Turonian organic facies in the western Mediterranean and along the adjacent Atlantic margin, in *Deposition of Organic Facies*, *Stud. Geol.*, vol. 40, edited by A. Y. Huc, pp. 133–160, Am. Assoc. Petrol. Geol., Tulsa, Okla.

Kuypers, M. M. M., R. D. Pancost, and J. S. Sinninghe Damsté (1999), A large and abrupt fall in atmospheric CO_2 concentration during Cretaceous times, *Nature*, *399*, 342–345.

Kuypers, M. M. M., R. D. Pancost, I. A. Nijenhuis, and J. S. Sinninghe Damsté (2002), Enhanced productivity led to increased organic carbon burial in the euxinic North Atlantic basin during the late Cenomanian oceanic anoxic event, *Paleoceanography*, *17*(4), 1051, doi:10.1029/2000PA000569.

Larson, R. L. (1991), Geological consequences of superplumes, *Geology*, *19*, 963–966.

Lea, D. W., T. A. Mashiotta, and H. J. Spero (1999), Controls on magnesium and strontium uptake in planktonic foraminifera determined by live culturing, *Geochim. Cosmochim. Acta*, *63*, 2369–2379.

Leckie, R. M., J. I. Kirkland, and W. P. Elder (1997), Stratigraphic framework and correlation of a principal reference section of the Mancos Shale (upper Cretaceous), Mesa Verde, Colorado, in *New Mexico Geological Society Guidebook*, *48th Field Conference: Mesozoic Geology and Paleontology of the Four Corners Region*, pp. 163–216, N. M. Geol. Soc., Las Cruces, N. M.

Lowenstam, H. A. (1961), Mineralogy, O^{18}/O^{16} ratios, and strontium and magnesium contents of recent and fossil brachiopods and their bearing on the history of the oceans, *J. Geol.*, *69*, 241–260.

Luderer, F., and W. Kuhnt (1997), A high resolution record of the *Rotalipora* extinction in laminated organic-carbon rich limestones of the Tarfaya Atlantic coastal basin (Morocco), *Ann. Soc. Géol. Nord*, *5*, 199–205.

Machel, H. G., R. A. Mason, A. N. Mariano, and A. Mucci (1991), Causes and emission of luminescence in calcite and dolomite, in *Luminescence Microscopy: Quantitative and Qualitative Aspects, SEPM Short Course*, vol. 25, edited by C. E. Barker and O. C. Kopp, pp. 9–25, Soc. for Sediment. Geol., Tulsa, Okla.

Miller, K. G., E. Barrera, R. K. Olsson, P. J. Sugarman, and S. M. Savin (1999), Does ice drive early Maastrichtian eustasy?, *Geology*, *27*, 783–786.

Miller, K. G., P. J. Sugarman, J. V. Browning, M. A. Kominz, J. C. Hernández, R. K. Olsson, J. D. Wright, M. D. Feigenson, and W. Van Sickel (2003), Late Cretaceous chronology of large, rapid sea-level changes: Glacioeustasy during the greenhouse world, *Geology*, *31*, 585–588.

Millero, F. J., and A. Poisson (1981), International one-atmosphere equation of state for sea water, *Deep Sea Res. Part A*, *28*, 625–629.

Morrison, J. O., and U. Brand (1986), Geochemistry of recent marine invertebrates, *Geosci. Can.*, *13*, 237–254.

Norris, R. D., K. L. Bice, E. A. Magno, and P. A. Wilson (2002), Jiggling the tropical thermostat in the Cretaceous hothouse, *Geology*, *30*, 299–302.

Orth, C. J., M. Attrep Jr., L. R. Quintana, W. P. Elder, E. G. Kauffman, R. Diner, and T. Villamil (1993), Elemental abundance anomalies in the late Cenomanian extinction interval: A search for the source(s), *Earth Planet. Sci. Lett.*, *117*, 189–204.

Otto-Bliesner, B. L., E. C. Brady, and C. Shields (2002), Late Cretaceous ocean: Coupled simulations with the National Center for Atmospheric Research Climate System Model, *J. Geophys. Res.*, *107*(D2), 4019, doi:10.1029/2001JD000821.

Paul, C. R. C., S. F. Mitchell, J. D. Marshall, P. N. Leary, A. S. Gale, A. M. Duane, and P. W. Ditchfield (1994), Palaeoceanographic events in the middle Cenomanian of northwest Europe, *Cretaceous Res.*, *15*, 707–738.

Paul, C. R. C., M. A. Lamolda, S. F. Mitchell, M. R. Vaziri, A. Gorostidi, and J. D. Marshall

(1999), The Cenomanian-Turonian boundary at Eastbourne (Sussex, UK): Aa proposed European reference section, *Palaeogeogr. Palaeoclimatol. Palaeoecol.*, *150*, 83–121.

Peck, L. S. (2001), Ecology of articulated brachiopods, in *Brachiopods Ancient and Modern*, *Paleontol. Soc. Pap.*, vol. 7, edited by S. Carlson and M. R. Sandy, pp. 171–183, Paleontol. Soc., New Haven, Ct.

Pitman, W. C., and X. Golovchenko (1983), The effect of sea-level change on the shelfedge and slope of passive margins, in *The Shelfbreak: Critical Interface on Continental Margins*, *Soc. Econ. Paleontol. Mineral. Spec. Publ.*, vol. 33, edited by D. J. Stanley and G. T. Moore, pp. 41–58, Soc. for Sediment. Geol., Tulsa, Okla.

Pletsch, T., J. Erbacher, A. E. L. Holbourn, W. Kuhnt, M. Moullade, F. E. Oboh-Ikuenobede, E. Söding, and T. Wagner (2001), Cretaceous separation of Africa and South America: The view from the West African margin (ODP Leg 159), *J. S. Am. Earth Sci.*, *14*, 147–174.

Poulsen, C. J., E. J. Barron, W. H. Peterson, and P. A. Wilson (1999), A reinterpretation of mid-Cretaceous shallow marine temperatures through model-data comparison, *Paleoceanography*, *14*, 679–697.

Poulsen, C. J., E. J. Barron, M. A. Arthur, and W. H. Peterson (2001), Response of the mid-Cretaceous global oceanic circulation to tectonic and CO2 forcing, *Paleoceanography*, *16*, 576–592.

Poulsen, C. J., A. S. Gendaszek, and R. L. Jacob (2003), Did rifting of the Atlantic Ocean cause the Cretaceous thermal maximum?, *Geology*, *31*, 115–118.

Sageman, B. B., M. A. Arthur, G. E. Birchfield, and W. E. Dean (1997), Evidence for Milankovitch periodicities in Cenomanian-Turonian lithologic and geochemical cycles, western interior USA, *J. Sediment. Res.*, *67*, 286–302.

Sahagian, D., and M. Jones (1993), Quantified middle Jurassic to Paleogene eustatic variations based on Russian platform stratigraphy: Stage-level resolution, *Geol. Soc. Am. Bull.*, *105*, 1109–1118.

Sahagian, D. L., A. L. Beisel, and V. A. Zakharov (1994), Sequence stratigraphy enhancement of biostratigraphic correlation with application to the upper Cretaceous of northern Siberia: A potential tool for petroleum exploration, *Intern. Geol. Rev.*, *36*, 359–372.

Schlanger, S. O., and H. C. Jenkyns (1976), Cretaceous oceanic anoxic events: Causes and consequences, *Geol. Mijnbouw*, *55*, 179–184.

Scholle, P. A., and M. A. Arthur (1980), Carbon isotope fluctuations in Cretaceous pelagic limestones: Potential stratigraphic and petroleum exploration tool, *AAPG Bull.*, *64*, 67–87.

Schouten, S., E. C. Hopmans, A. Forster, Y. van Breugel, M. M. M. Kuypers, and J. S. Sinninghe Damsté (2003), Extremely high sea-surface temperatures at low latitudes during the middle Cretaceous as revealed by archael membrane lipids, *Geology*, *31*, 1069–1072.

Shackleton, N. J. (1974), Attainment of isotopic equilibrium between ocean water and the benthonic foraminifera Genus *Uvigerina*: Isotopic changes in the ocean during the last glacial, *Colloq. Int. C. N. R. S.*, *219*, 4–5.

Shackleton, N. J., and J. P. Kennett (1975), Paleotemperature history of the Cenozoic and initiation of Antarctic glaciation: Oxygen and carbon isotope analysis in DSDP sites 277, 279 and 281, *Initial Rep. Deep Sea Drill. Project*, *29*, 743–755.

Sinton, C. W., and R. A. Duncan (1997), Potential links between ocean plateau volcanism and global ocean anoxia at the Cenomanian-Turonian Boundary, *Econ. Geol.*, *92*, 836–842.

Stanley, S. M., and L. A. Hardie (1998), Secular oscillations in the carbonate mineralogy of reef-building and sediment producing organisms driven by tectonically forced shifts in seawater chemistry, *Palaeogeogr. Palaeoclimatol. Palaeoecol.*, *144*, 3–19.

Steuber, T. (2002), Plate tectonic control on the evolution of Cretaceous platform-carbonate production, *Geology*, *30*, 259–262.

Steuber, T., and J. Veizer (2002), Phanerozoic record of plate tectonic control of seawater chemistry and carbonate sedimentation, *Geology*, *30*, 1123–1126.

Stoll, H. M., and D. P. Schrag (1998), Effects of Quaternary sea level cycles on strontium in seawater, *Geochim. Cosmochim. Acta*, *62*, 1107–1118.

Stoll, H. M., and D. P. Schrag (2000), High-resolution stable isotope records from the upper Cretaceous rocks of Italy and Spain: Glacial episodes in a greenhouse planet?, *Geol. Soc. Am. Bull.*, *112*, 309–319.

Stoll, H. M., and D. P. Schrag (2001), Sr/Ca variations in Cretaceous carbonates: Relation to productivity and sea level change, *Palaeogeogr. Palaeoclim. Palaeoecol.*, *168*, 311–336.

Summerhayes, C. P. (1987), Organic-rich Cretaceous sediments from the North Atlantic, *Geol. Soc. Spec. Publ.*, *26*, 301–316.

Tucholke, B. E., and P. R. Vogt (1979), Western North Atlantic: Sedimentary evolution and aspects of tectonic history, *Initial Rep. Deep Sea Drill. Project*, *43*, 791–826.

Veizer, J. (1983), Chemical diagenesis of carbonates: Theory and application of trace element technique, in *Stable Isotopes in Sedimentary Geology, Short Course*, vol. 10, edited by M. A. Arthur, pp. 3.1–3.100, Soc. for Sediment. Geol., Tulsa, Okla.

Veizer, J., P. Fritz, and B. Jones (1986), Geochemistry of brachiopods: Oxygen and carbon isotopic records of Paleozoic oceans, *Geochim. Cosmochim. Acta*, *50*, 1679–1696.

Voigt, S. (2000), Cenomanian-Turonian composite $\delta^{13}C$ curve for western and central Europe—The role of organic and inorganic carbon fluxes, *Palaeogeogr. Palaeoclimatol. Palaeoecol.*, *160*, 91–104.

Voigt, S., and H. Hilbrecht (1997), Late Cretaceous carbon isotope stratigraphy in Europe: Correlation and relations with sea level and sediment stability, *Palaeogeogr. Palaeoclimatol. Palaeoecol.*, *134*, 39–60.

Voigt, S., and F. Wiese (2000), Evidence for late Cretaceous (late Turonian) climate cooling from oxygen-isotope variations and palaeobiogeograpic changes in western and central Europe, *J. Geol. Soc.*, *157*, 737–744.

Voigt, S., M. Wilmsen, R. N. Mortimore, and T. Voigt (2003), Cenomanian palaeotemperatures derived from the oxygen isotopic composition of brachiopods and belemnites: Evaluation of Cretaceous palaeotemperature proxies, *Geol. Rundsch.*, *92*, 285–299.

Walaszczyk, I., and W. A. Cobban (2000), *Inoceramid Faunas and Biostratigraphy of the Upper Turonian-Lower Coniacian of the Western Interior of the United States*, *Spec. Pap. Palaeontol.*, vol. 64, Palaeontol. Assoc., London.

Wallmann, K. (2001), The geological water cycle and the evolution of marine $\delta^{18}O$ values, *Geochim. Cosmochim. Acta*, *65*, 2469–2485.

Wiese, F., S. Voigt, S. Cech, and M. Kostak (2004), The upper Turonian of the Bohemian Cretaceous Basin (Czech Republic) exemplified by the Úpohlavy working quarry: Integrated stratigraphy and palaeoceanography of a gateway to the Tethys, *Cretaceous Res.*, *25*, 329–352.

Wilmsen, M. (2003), Sequence stratigraphy and palaeoceanography of the Cenomanian Stage in northern Germany, *Cretaceous Res.*, *24*, 525–568.

Wilmsen, M., F. Wiese, and G. Ernst (1996), Facies development, events and sedimentary sequences in the Albian to Maastrichtian of the Santander depositional area, northern Spain, *Mitt. Geol. Paläontol. Inst. Univ. Hamburg*, *77*, 337–367.

Wilson, P., and R. D. Norris (2001), Warm tropical ocean surface and global anoxia during the mid-Cretaceous period, *Nature*, *412*, 425–429.

Wilson, P. A., R. D. Norris, and M. J. Cooper (2002), Testing the Cretaceous greenhouse hypothesis using glassy foraminiferal calcite from the core of the Turonian tropics on Demerara Rise, *Geology*, *30*, 607–610.

Wold, C. N. (1995), Palaeobathymetric reconstruction on a gridded database: The northern North Atlantic and southern Greenland-Iceland-Norwegian Sea, *Geol. Soc. Spec. Publ.*, *90*, 271–302.

Wray, D. S. (1999), Identification and long-range correlation of bentonites in Turonian-Coniacian (upper Cretaceous) chalks of northwest Europe, *Geol. Mag.*, *136*, 361–371.

Zachos, J., L. D. Stott, and K. C. Lohman (1994), Evolution of early Cenozoic marine temperatures, *Paleoceanography*, *9*, 353–387.

Zakharov, V. A., A. L. Beisel, N. K. Lebedeva, and O. V. Khomentovskiy (1991), Svidetelystva evstatiki mirovogo okeana v verkhnem mely na severe Sibiri, *Akad. Nauk SSSR*, *8*, 8–15.

Zeebe, R. E. (2001), Seawater pH and isotopic paleotemperatures of Cretaceous oceans, *Palaeogeogr. Palaeoclimatol. Palaeoecol.*, *170*, 49–57.

S. Flögel, Leibnitz-Institut für Meereswissenschaften, Wischhofstr. 1-3, D-24148 Kiel, Germany. (sfloegel@ifm-geomar.de)

A. S. Gale, Department of Palaeontology, Natural History Museum, SW7 5BD London, UK. (asg@nhm.ac.uk)

S. Voigt, Geological Institute, University of Cologne, Zülpicher Str. 49a, D-50674 Köln, Germany. (silke.voigt@uni-koeln.de)